COMPREHENSIVE REVIEW OF COLLECTED NOISE INFORMATION AT BARRIER SITES

UCF Project No. 16 21 740
Agency No. BC355/RPW07

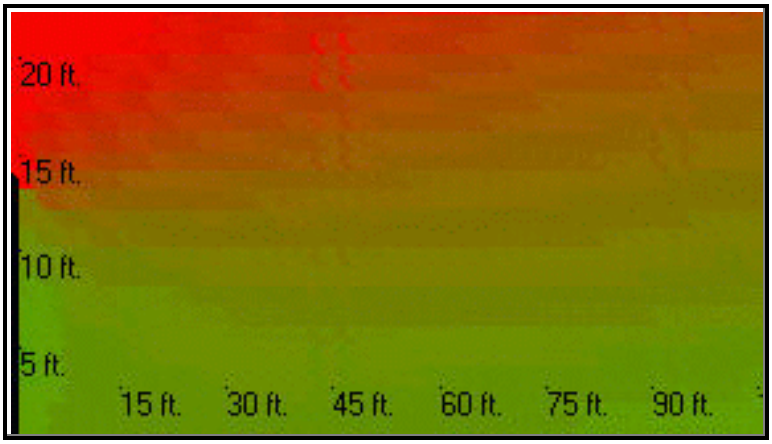

Submitted to:
The Florida Department of Transportation
605 Suwannee Street
Tallahassee, Florida 32299-0450

Prepared by:

The University of Central Florida
Community Noise Laboratory
Civil & Environmental Engineering Department
P.O. Box 162450
Orlando, Florida 32816-2450

October 7, 2003

DISCLAIMER

Technical Report Documentation Page

1. Report No.	2. Government Accession No.	3. Recipient's Catalog No.
BC355/RPW07		

4. Title and Subtitle	5. Report Date
COMPREHENSIVE REVIEW OF COLLECTED NOISE INFORMATION AT BARRIER SITES	October 7, 2003
	6. Performing Organization Code
7. Author(s)	8. Performing Organization Report No.
R.L.Wayson, J.M. MacDonald, A. El-Aassar, C.B. Chua	16-21-740
9. Performing Organization Name and Address	10. Work Unit No. (TRAIS)
University of Central Florida Community Noise Lab: Civil & Environmental Engineering Orlando, Florida 32816-2450	11. Contract or Grant No. BC355
12. Sponsoring Agency Name and Address	13. Type of Report and Period Covered
Florida Department of Transportation **605 Suwannee St. MS 30** **Tallahassee, Florida 32399** **(850)414-4615**	**Final Report**
	14. Sponsoring Agency Code

15. Supplementary Notes

Prepared in cooperation with the USDOT and FHWA

16. Abstract

This report describes the results of a detailed analysis of in-situ measurements for 19 noise barriers in the State of Florida. This report is a continuation of work presented in two previous Florida Department of Transportation (FDOT) reports, which are described in the introduction. This report investigates, in greater detail, the substantial database produced by this project. This investigation evaluated spectral differences of predicted and measured ground effects and high frequency deviations between federal prediction methods compared to measured data. This work also produced custom software that provided a visualization of the formation of shadow zones behind existing barriers. In addition, new empirical methods were developed to estimate the length of shadow zones behind highway noise barriers. This software should can lead to more effective design of future highway noise barriers.

17. Key Word	18. Distribution Statement
	No Restriction **This report is available to the public through the NTIS, Springfield, VA 22161**

19. Security Classif. (of this report)	20. Security Classif. (of this page)	21. No. of Pages	22. Price
Unclassified	**Unclassified**	71	

Form DOT F 1700.7 (8-72) Reproduction of completed page authorized

EXECUTIVE SUMMARY

This report describes the results of a detailed analysis of in-situ measurements of 19 noise barriers in the state of Florida. This work is a continuation of work presented in two previous Florida Department of Transportation (FDOT) reports which are briefly described in the Introduction. This report investigates, in greater detail, the substantial database produced by this project. This investigation evaluated spectral differences of predicted and measured ground effects and high frequency deviations between federal prediction methods compared to measured data. This work also produced custom software that provided a visualization of the formation of shadow zones behind existing barriers. In addition, new empirical methods were developed to estimate the length of shadow zones behind highway noise barriers which can lead to more effective design of future highway noise barriers.

This work has provided an in-depth look at the effectiveness of the noise barriers in Florida. It has allowed a closer look at the modeling process and has developed software to visualize and estimate shadow zones behind barriers. Important results of this work include the following:

- A new empirical method of predicting shadow zone length behind barriers was developed and requires information readily available to a DOT planner. This method provides a convenient way to estimate shadow zone length based on actual measurements that include background sound level contribution.
- A new method of background source allocation was developed and used in development of the shadow zone length model.
- TNM predicted reference spectra, above the barrier) were similar to measured spectra.
- An average error of 1 dB(A) was observed in the TNM predicted ‘ground dip’ but the source of the error is unclear but thought to be due to the angle of the sound wave and the ground plane. A value of about 10 cgs Rayls provided a better fit with measured results than did the default ‘lawn’ ground type (300 cgs Rayls).
- High frequency effects, caused by refraction (meteorological effects) are not considered in most traffic noise prediction models and this leads to differences between predicted and measured high frequency spectra. However, the effects are small and would seem not to be a primary concern for calm winds and short distances at this time.
- Software was developed to allow visualization of the soundscape and shadow zone behind barriers. This software is being provided to FDOT for use in design of highway noise barriers in Florida.

TABLE OF CONTENTS

LIST OF TABLES

LIST OF FIGURES

I. OVERVIEW

This report describes the results of detailed analysis of in-situ measurements of 19 noise barriers in the state of Florida. This report is a continuation of work presented in two previous Florida Department of Transportation (FDOT) reports which are described in the introduction. This report investigates, in greater detail, the substantial database produced by this project. This investigation evaluated spectral differences of predicted and measured ground effects and high frequency deviations between federal prediction methods compared to measured data. This work also produced custom software that provided a visualization of the formation of shadow zones behind existing barriers. In addition, new empirical methods were developed to estimate the length of shadow zones behind highway noise barriers which can lead to more effective design of future highway noise barriers.

The goals of this project were the following:

1. Compare the 1/3 octave band data to that in TNM to gain further insight into the narrowband capabilities of TNM. A special version of TNM that reports 1/3 octave band results will be used for this project.

2. Continue development of a 'shadow zone length' model that determines the extent of the shadow zone behind a barrier, given site specific parameters.

3. Evaluate TNM prediction accuracy when using actual meteorological site conditions rather than default FHWA values.

II. INTRODUCTION

Parts 1 and 2 of this project [1][2] described sound pressure levels measured above and behind nineteen noise barrier sites in the state of Florida. The previous work described the measurement procedures and methodology in detail, summarized the L_{eq} levels measured at the nineteen sites and also assessed the accuracy of Federal highway noise prediction models when compared to these actual measurements. This resulted in several findings that included:

1. Florida barriers most often provide a 5-10 dB benefit to 1st row receivers.

2. TNM often, but not always, predicts greater insertion losses than versions 2.0 and 2.1 of STAMINA. This is thought to be directly related to TNM continuing to predict ground effects in presence of a taller noise barrier, while STAMINA does not.

3. TNM outperformed STAMINA 2.0 and STAMINA 2.1 in prediction of the absolute sound

levels and the propagation losses from the barrier to locations behind the barrier.

4. Shadow zones benefits, as determined by a 5 dB: L_{Aeq} sound level reduction, generally were limited to under 400 feet (122 meters) behind even the taller noise barriers.

5. The use of the "OGAC" input type provided better results in Florida when using the FHWA TNM model. This is expected since Florida uses an open-graded friction mix. Although pavement type at this time should not be used as an abatement measure, appropriate pavement type should be permitted to reduce TNM prediction errors.

6. An empirical relation was developed to estimate shadow zone length and benefitted receivers. This approximate method allows for a better understanding of homes actually receiving benefits since it accounts for background sound levels that are ignored in existing computer models.

Table 1 contains a summary of the noise barriers tested for this project. Measurements were conducted with careful regard to published procedures [3][4][5]. The final insertion loss reported were determined using the indirect method prescribed by American National Standards Institute (ANSI) [4]. The estimated lengths of the shadow zone shown in Table 1 were determined using an earlier method derived by the research team. The method has been refined and is discussed in detail later in the paper.

Figure 1 depicts the standard microphone positions used at each barrier location. These microphone positions are defined by the ANSI standard [4] for determination of the indirect insertion loss of an in-situ barrier. There were several cases where sound levels were measured and recorded at distances further than those noted in Figure 1 ('rover' sites). These rover site measurements were used to estimate the edge of the shadow zone created by the barrier.

The effectiveness of the barrier was evaluated by placing the primary emphasis on the receiver locations at a height of 5 feet (1.5 meters) above the ground plane. These were microphone locations 1, 4, A, B, C and D. All rover microphones were also placed at five feet (1.5 meters) above the local ground plane and used in the shadow zone length determination. Significant barrier attenuation was assumed to occur if at least 5 dB:L_{Aeq} of insertion loss (noise reduction after the barrier is constructed compared to the no-barrier case) occurred. A 5 dB:L_{Aeq} reduction in noise levels represents a perceptible change in the soundscape for most individuals. This is in accordance with FDOT policy as stated in Chapter 17 of the Project Development and Environmental Manual [6] where a benefitted receiver is defined as:

> "A benefitted receiver is a noise sensitive receiver that will obtain a minimum of 5 dBA of noise reduction as a result of the use of a specific noise abatement activity regardless of whether or not they are identified as impacted. Only benefitted receivers will be included in the calculation needed to determine that any particular noise abatement scheme has a reasonable cost."

Table 1. ANSI Adjusted Insertion Loss for All Sites.

Site	Major Source	Effective Wall Height	ANSI IL at 15 meters	ANSI IL at 30 meters	Length of Shadow Zone
A. Jacksonville	I-95	18.5 ft. (5.6 m)	--	7	210 ft. (64 m)
B. Jacksonville	I-295	13.5ft. (4.1 m)	8	5	141 ft. (43 m)
C. Daytona Beach	S.R. 5A	14.5 ft. (4.4 m)	10	9	254 ft. (77 m)
E. Brandon	I-75	41.0 ft. (12.5 m)	2	8	362 ft. (110 m)
F. Clearwater	S.R. 636	11.0 ft. (3.4 m)	6	3	130 ft. (40 m)
G. St. Petersburg	S.R. 682	7.3 ft. (2.2 m)	5	3	73 ft. (22 m)
H. Ft. Lauderdale	I-95	14.5 ft. (4.4 m)	9	9	243 ft. (74 m)
I. Deerfield Beach	I-95	13.1 ft. (4.0 m)	6	5	150 ft. (46 m)
J. Miami	I-195	18.0 ft. (5.5 m)	6	5	90 ft. (27m)
K. Tamiami	U.S. 41	11.0 ft. (3.4 m)	11	7	--
L. Hialeah	S.R. 924	25.3 ft. (7.7 m)	7	7	171 ft. (52 m)
M. Wildwood	S.R. 44	9.4 ft. (2.9 m)	9	9	320 ft. (97 m)
N. Maitland	S.R. 414	11.6 ft. (3.5 m)	7	5	157 ft. (48 m)
O. Ft. Lauderdale (H. Repeat)	I-95	14.5 ft. (4.4 m)	10	9	316 ft. (96 m)
P. Ft. Lauderdale	I-95	18.4 ft. (5.6 m)	12	10	445 ft. (136 m)
Q. West Palm Beach	I-95	19.3 ft. (5.9 m)	14	9	390 ft. (119 m)
R. Palm Harbor, Tampa	S.R. 586	7.7 ft. (2.3 m)	7	7	251 ft. (76 m)
S. New Port Richey	S.R. 54	11.0 ft. (3.4 m)	9	7	305 ft. (93 m)
T. Longwood (wood fence)	I-4	NA	--	--	no barrier

* *Barrier height is the height above ground at the base of the barrier while effective height is the height above the receiver ground plane*.

Substantial noise reduction in this report again relies on FDOT guidance and is defined as:

> "This is an effort to reduce traffic noise impacts at benefitted receptors by 10 decibels or more if possible, with a minimal acceptable level of reduction at no less than 5 decibels."

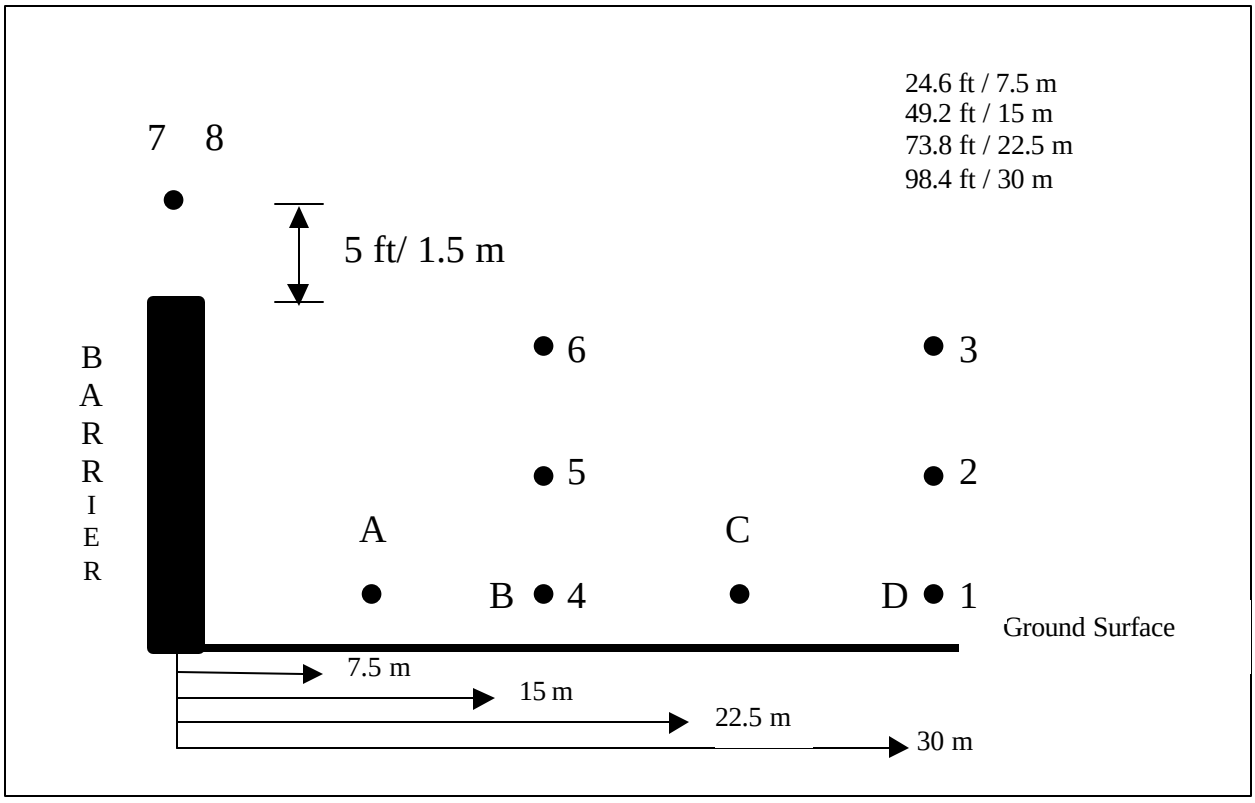

Figure 1. Microphone Positions and Naming Convention.

III. OBJECTIVE AND METHODOLOGY OF LATEST WORK

The latest work involved a closer inspection of the sound pressure level data collected during this research and included a more detailed analysis of the third octave band data. The data analysis of Parts 1 and 2 was primarily concerned with the broadband 'A' weighted L_{eq} sound levels and sought to draw general conclusions about barrier effectiveness and federal prediction method accuracy. This latest work describes a new shadow zone length estimation method and investigates frequency dependent items such as ground effects and atmospheric effects.

This paper contains two major sections, the first takes a detailed look at the narrowband data collected during this project and discusses the ground effect and atmospheric effects measured at the sites and compares them to spectra predicted by the Federal Highway Administration (FHWA) Traffic Noise Model (TNM). The second section discusses a new method to estimate shadow zone length behind barriers. This method was developed from the data measured during this project and is important since it gives valuable information into the true effectiveness of a barrier that includes information such as background sound levels. The FHWA traffic noise prediction models do not have a provision for background noise and this can lead to overestimation of the barrier effectiveness and length of the shadow zone for a proposed barrier.

IV. TNM 1/3 OCTAVE BAND RESULTS

A. Low/Mid Frequency Deviations: Ground Effects

Microphone positions 1 and 4 (see Figure 1) were chosen to evaluate ground effects since they are near the ground at a height typical of normal receiver locations used to estimate outdoor impacts. Microphone positions A and C were broadband locations and did not include 1/3 octave band data. TNM 1/3 octave band results were compared to the measured L_{eq} spectral data at positions 1 and 4. The location and magnitude of the 'ground dip' was investigated. The 'ground dip' is the result of direct sound waves interacting with waves interacting with an absorptive boundary surface. TNM results and measured data were ($L_{Aeq,1hr}$) plotted against the spectrum of the reference sound level (five feet above top of the wall) and normalized with respect to 1000 Hz band. Normalization provides an easier visual comparison of the TNM predicted spectra versus the measured spectra.

Table 2 shows the results of the investigation comparing the measured results to TNM. TNM results show that in general, the ground dip tended to begin at 200 Hz and ended near 500 Hz. Conversely, the measured data indicates that the dip begins around 80 Hz to 100 Hz and ends from 200 to 315 Hz depending on the geometry of the site. Figure 2 contains examples of the measured and TNM predicted ground dip for sites G and I. The figures show the presence of the measured ground dip is broad and shallow for these sites while the TNM predicted ground dip is more narrow and pronounced. Table 2 and Figure 2 show that the TNM predicted ground dip is essentially constant, regardless of site geometry and is more pronounced than the measured ground dip for these barrier sites. This is a qualitative statement but of more interest is the quantitative difference in the broadband level between the measured data and the TNM predicted band levels.

Table 3 is a summary of the computed 'A' weighted sound level for microphones 1 and 4 after normalization at the 1000 Hz. band. The difference between the measured and predicted values in this case provides an indication of the ground dip error. The full spectra results of Table 4 are the results that would be reported to the TNM user. Tables 3 and 4 summarizes the ground dip error over the frequency range of the measured ground dip. The sound levels shown in the table were computed according to the following equation:

$$SPL_{broadband} = 10 * \log_{10} \sum_{freq_{startofdip}}^{freq_{endofdip}} 10^{(SPL_{freq}/10)} \qquad (1)$$

where:
$freq_{startofdip}$ = frequency where ground dip starts
$freq_{endofdip}$ = frequency where ground dip ends
SPL_{freq} = pressure level at one third octave band

Table 2. 'Ground Dip' Phenomena Frequency Range.

Site	Measured dip (Mic. 1), Hz	TNM dip (Mic. 1), Hz	Measured dip (Mic. 4), Hz	TNM dip (Mic. 4), Hz
A	100-315	200-500	---	---
B	80-250	200-500	80-250	200-500
C	100-315	200-400	100-315	200-400
E	100-200	200-500	80-200	200-500
F	125-315	200-500	100-315	200-500
G	100-250	200-500	250-400	200-500
H	80-200	200-400	80-315	200-400
I	80-250	200-500	80-250	200-400
J	80-315	200-400	80-250	200-500
K	80-315	200-500	80-315	200-400
L	80-200	200-400	100-250	200-400
M	100-315	200-630	100-315	200-500
N	63-160	200-630	80-250	200-500
O	80-400	200-500	80-315	200-400
P	160-400	200-500	125-250	200-500
Q	80-315	200-500	80-250	200-500
R	---	---	125-250	200-400
S	80-400	200-400	80-400	200-400
T	125-400	200-400	125-400	200-400

The start and end frequencies referred to in Equation (1) and shown in Table 3 are listed in Table 2. The last entry in Tables 3 and 4 is the average error of the residual between the measured sound level in the dip frequency range. Table 3 shows that the TNM predicted sound level (broadband), on average, is over-predicting by about 1 dB(A) for microphone positions 1 and 4 due to the error in ground dip prediction. This is not considered to be a dramatic prediction error for traffic noise modeling but could make a big difference on determining benefitted receivers and in the determination of receivers approaching or exceeding the Noise Abatement Criteria.

Figure 2. Partial Spectra Plots of Ground Effect Errors (Normalized).

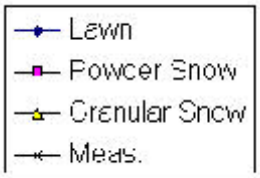

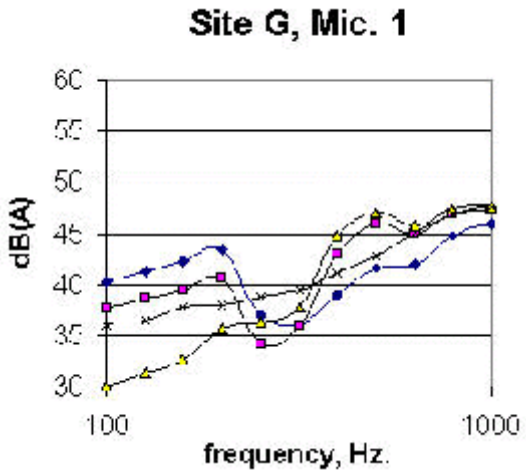

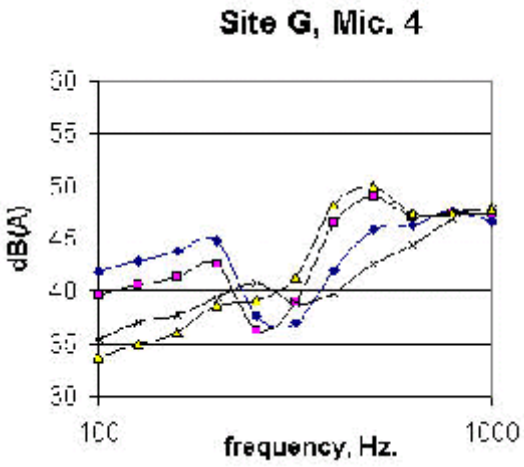

Figure 2. Partial Spectra Plots of Ground Effect Errors (Normalized).

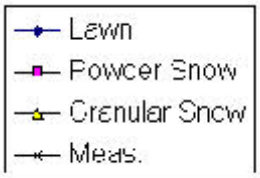

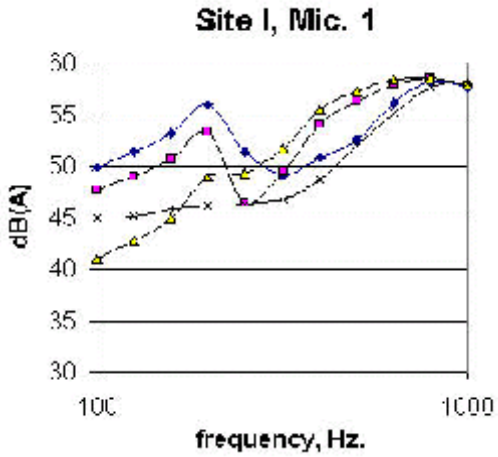

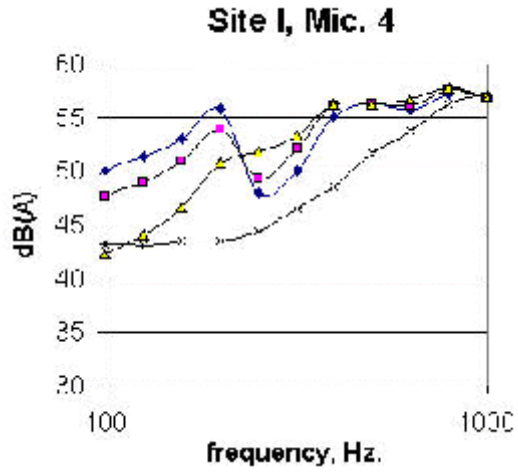

Table 3. Full Spectra Error Results (TNM - Measured).

Site	mic 1	abs(mic 1)	mic 4	abs(mic 4)
A	2.1	2.1	--	--
B	1.4	1.4	1.8	1.8
C	-0.8	0.8	-0.4	0.4
E	0.3	0.3	-0.5	0.5
F	2.8	2.8	1.6	1.6
G	0.6	0.6	2.0	2.0
H	1.0	1.0	2.1	2.1
I	2.3	2.3	2.8	2.8
J	1.1	1.1	1.1	1.1
K	0.0	0.0	1.9	1.9
L	3.2	3.2	2.2	2.2
M	0.2	0.2	0.9	0.9
N	0.3	0.3	0.6	0.6
O	2.1	2.1	2.8	2.8
P	0.4	0.4	2.0	2.0
Q	1.2	1.2	1.3	1.3
R	--	--	0.8	0.8
S	0.1	0.1	1.2	1.2
T	-0.8	0.8	-0.4	0.4
avg	**1.0**	**1.1**	**1.3**	**1.5**
stdev	**1.2**	**1.0**	**1.0**	**0.8**

An explanation of the TNM error associated with microphones 1 and 4 could be the effect of the increased incident angle from the imaginary source at the top of the barrier versus the grazing incidence assumed by the TNM ground effect algorithm. However, without the source code, there is no direct way to test the diffraction routine other than varying geometrical site parameters. The error could be in other parts of the TNM diffraction routine. It is possible, however, to perform tests of the ground effect routine and to gain insight into its performance relative to these measured sound levels and base preliminary findings on these results. The ground effect algorithm used by TNM computes the impedance of the ground surface based on the user defined effective flow resistivity (efr, cgs Rayls) of the ground. This efr value is used to calculate the impedance of the ground surface based on the results of Delany and Bazley [7]. The Delany and Bazley impedance model equations are repeated below.

Table 4. Partial Spectra Error Results (TNM - Measured).

site	mic 1	abs(mic 1)	mic 4	abs(mic 4)
A	8.3	8.3	--	--
B	5.7	5.7	5.7	5.7
C	1.5	1.5	0.2	0.2
E	5.7	5.7	8.0	8.0
F	10.1	10.1	6.1	6.1
G	5.4	5.4	0.8	0.8
H	5.6	5.6	5.8	5.8
I	7.3	7.3	8.8	8.8
J	5.3	5.3	5.5	5.5
K	4.4	4.4	5.1	5.1
L	7.2	7.2	5.3	5.3
M	3.3	3.3	3.5	3.5
N	7.2	7.2	5.4	5.4
O	3.7	3.7	6.4	6.4
P	0.3	0.3	5.1	5.1
Q	3.1	3.1	5.0	5.0
R	--	--	3.9	3.9
S	3.5	3.5	4.4	4.4
T	-5.0	5.0	-4.0	4.0
avg	**4.6**	**4.9**	**4.5**	**4.9**
stdev	**3.4**	**2.6**	**3.0**	**2.1**

$$Z = R + iX \tag{2}$$

$$\mathrm{Re}(Z_2/Z_1) = R = 1 + 9.08\,(f/s)^{-0.75} \tag{3}$$

$$\mathrm{Im}(Z_2/Z_1) = X = 11.9\,(f/s)^{-0.73} \tag{4}$$

f = frequency, Hz
s = effective flow resistivity (efr), cgs Rayls
Z_2 = impedance of second medium (ground)
Z_1 = impedance of first medium (air)

Equation 2 shows that the normalized complex ground impedance, Z, is dependent on the effective flow resistivity (efr) and the frequency of the sound wave but not dependent on the incident angle. This seems contrary to experience, one expects that the relative impedance of the ground surface would increase as the incident angle approaches normal, or ninety degrees. The efr value remains a constant value in the ground effect algorithm whereas our data indicate that its value becomes smaller as barrier height and incident angle increase.

The ground effect algorithm takes the incident angle into account with the reflection coefficient, R_p, shown in Equation (3).

$$R_p = \frac{\sin q_1 - \frac{Z_1}{Z_2}}{\sin q_1 + \frac{Z_1}{Z_2}} \qquad (5)$$

where: $?_1$ = incident angle of reflected sound wave

The reflection coefficient shown in Equation (5) is known as the locally reacting form of the reflection coefficient and it is clear that the reflection coefficient is dependent on the incident angle and the normalized ground impedance.

The idea that ground impedance changes as incident angle increases was tested by manually changing the effective flow resistivity in the TNM model and comparing predicted sound levels to the measured sound levels. This assumes that the TNM error is entirely located in the ground effect algorithm which was assumed and thought to be true, but cannot be proven without the source code. Bias due to source prediction errors has been minimized by normalizing the measured and predicted spectra at the 1000 kHz 1/3-octave band. The next section discusses the results of this testing.

B. TNM Tests of Different Ground Surfaces

The differences in the ground dip shape and depth led to investigation of ground type within the TNM model. Additional TNM input files were built with ground surface values other than the default "Lawn" (300 cgs Rayls) type. Table 5 shows the results of these additional tests. Table 5 contains the calculated error between the predicted and measured 'A' weighted, one hour Leq values for microphone locations 1 and 4 at each site using three different ground types, Lawn, Granular Snow (40 Rayls) and Powder Snow (10 Rayls). The TNM spectra were normalized to the measured value at 1 kHz to remove source prediction errors.

Table 5. Summary of Errors for Different TNM Ground Types, dB(A)

Site	Lawn (mic.1)	Granular Snow (mic.1)	Powder Snow (mic.1)	Lawn (mic.4)	Granular Snow (mic.4)	Powder Snow (mic.4)
A	2.1	1.5	1.2	--	--	--
B	1.4	1.5	1.4	1.7	1.2	0.8
C	-0.8	0.2	0.5	-0.4	-0.2	-0.4
E	0.4	-1.4	-2.1	-0.5	-1.3	-1.7
F	2.5	2.9	2.2	1.3	1.2	0.6
G	0.6	0.3	0.2	2.1	2.0	1.8
H	0.9	1.5	1.5	2.0	1.5	1.0
I	2.2	2.4	2.3	2.8	2.8	2.5
J	1.1	0.9	0.9	1.1	0.9	0.7
K	0.4	0.6	0.4	2.1	2.0	1.8
L	3.3	2.6	2.1	2.3	2.2	1.7
M	-0.2	-0.4	-0.5	0.6	-0.1	-0.4
N	0.3	1.1	1.3	0.6	0.8	0.7
O	1.9	2.5	2.5	2.6	1.9	1.4
P	0.3	-0.8	-1.1	1.8	1.4	0.8
Q	1.5	1.8	1.4	1.5	1.6	1.8
R	--	--	--	0.9	1.0	1.0
S	0.1	0.4	0.2	1.2	1.3	1.1
T	-0.6	-0.7	-0.7	-0.2	-0.2	-0.1

Tables 5 and 6 show that for most sites, the 'softer' ground surface provides a better fit to the measured $L_{eq,hr}$ spectra results for microphone 4. Six sites had improved error when modeled with a softer ground surface for microphone 1. At this point it is unclear if the ground effect algorithm and the imaginary source technique are in error or if other factors are causing the differences.

Table 6. Summary of Average Errors for Different TNM Ground Types, dB(A)

error	Lawn	Granular Snow	Powder Snow
Mic 1 avg. error	1.0	0.9	0.8
Mic 1 abs(error)	1.1	1.3	1.2
Mic 4 avg. error	1.3	1.1	0.8
Mic 4 abs(error)	1.4	1.3	1.1

Additional work was conducted to ensure that the ground dip differences were not simply transferred from the reference spectra to the microphone locations behind the wall. Figure 3 shows the reference spectra for sites E, F, I and L. The largest ground dip errors as indicated in the previous tables occurred at these sites.

Figure 3. Measured and Predicted Source Spectra (Not Normalized).

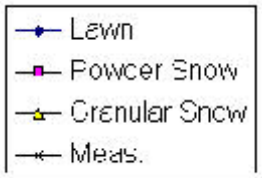

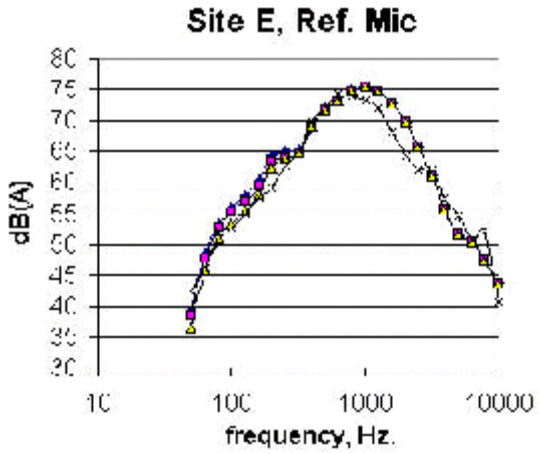

Figure 3. Measured and Predicted Source Spectra (Not Normalized).

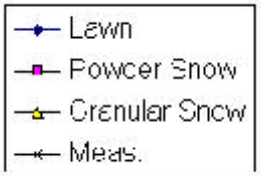

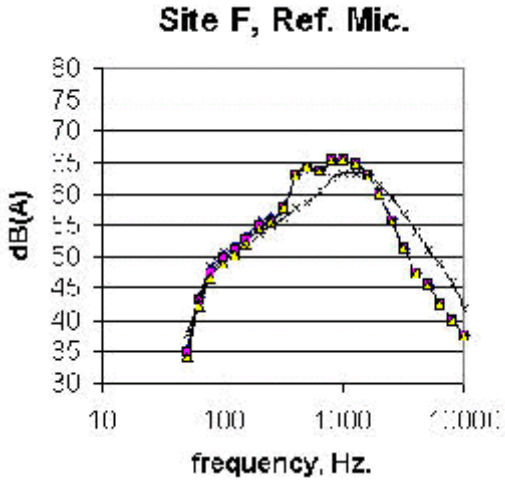

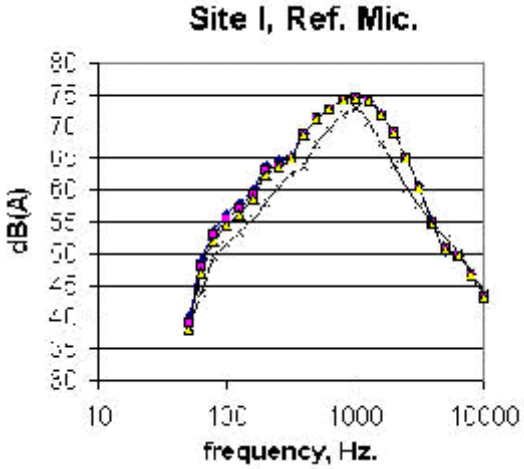

Figure 3. Measured and Predicted Source Spectra (Not Normalized).

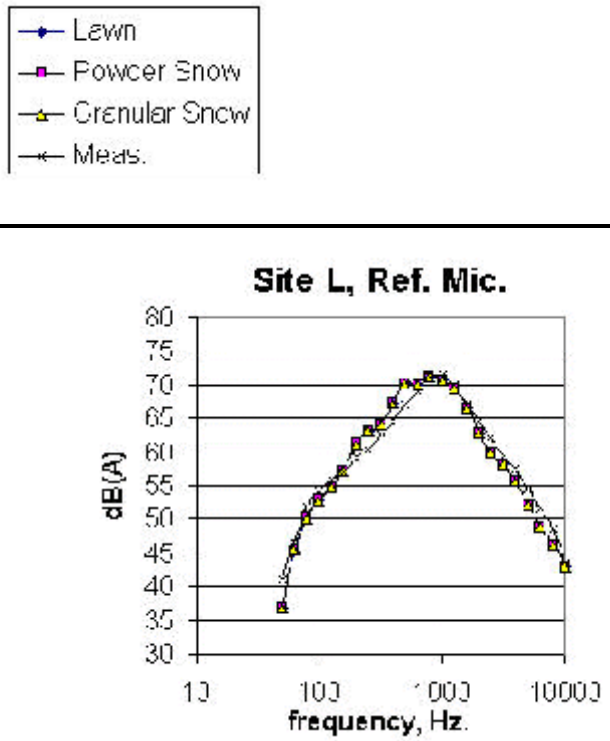

Figure 3 tends to indicate that the TNM predicted source spectra at the reference site, which is relatively unaffected by the ground effects, closely resembles the measured spectra for sites E, F, I and L which were the sites with the greatest ground dip error. This indicates that the ground dip error is real and not related to an incorrect source spectra from TNM. It should be noted that there are some differences between measured and predicted spectra in the range of 100 Hz. to 800 Hz. even at the reference site.

C. High Frequency Deviations: Atmospheric Effects

The previous section discussed trends and deviations, in the low to mid frequency range, between the measured data behind sound barriers and the computer models used to predict these levels. This section focuses on the higher frequencies and discusses some large deviations between measured and predicted sound levels.

Tables 7 and 8 are summaries of maximum errors between TNM spectra and measured spectra for

microphones 1 and 4 at the higher frequencies. Table 7 is a summary for microphone position 1 and it shows large errors at sites B, C, K and P. The table indicates that most of the errors occurred at the 5 kHz. frequency and were on the order of -10 to -20 dB (predicted - measured) for that band. Table 8 is a summary for microphone 4 and it shows large errors at sites B, C, H, N, Q and T.

Table 7. Observed High Frequency Differences Between Measured Data and TNM Predictions (Microphone Position 1).

Site	Maximum Deviation, dB(A)	Frequency	Range of Deviation
A	-12	5 kHz.	2kHz. - 10 kHz.
B	-17	10 kHz.	2kHz. - 10 kHz.
C	-20	10 kHz.	2kHz. - 10 kHz.
E	-10	5 kHz.	2kHz. - 8 kHz.
F	-3	2kHz.	2kHz. - 8 kHz.
G	-6	5 kHz.	3kHz. - 10 kHz.
H	-7	5 kHz.	3kHz. - 10 kHz.
I	-2	1500Hz.	1kHz. - 3 kHz.
J	-10	10kHz.	3kHz. - 10 kHz.
K	-15	5 kHz.	3kHz. - 10 kHz.
L	-4	5 kHz.	3kHz. - 10 kHz.
M	-5	5 kHz.	1kHz. - 10 kHz.
N	-10	5 kHz.	1kHz. - 10 kHz.
O	-5	5 kHz.	1kHz. - 10 kHz.
P	-17	5 kHz.	2kHz. - 10 kHz.
Q	-10	5 kHz.	3kHz. - 10 kHz.
S	-10	5 kHz.	1kHz. - 10 kHz.
T	-10	8 kHz.	3kHz. - 10 kHz.

Table 8. Observed High Frequency Differences Between Measured Data and TNM Predictions (Microphone Position 4).

Site	Maximum Deviation, dB(A)	Frequency	Range of Deviation
B	-17	5KHz.	2kHz. - 10 KHz.
C	-18	5kHz.	2kHz. - 10 kHz.
E	-10	5 kHz.	3kHz. - 10 kHz.
F	-10	5kHz.	1kHz. - 10 kHz.
G	-7	5 kHz.	3kHz. - 10 kHz.
H	-20	10kHz.	2kHz. - 10 kHz.
I	-5	10kHz.	3kHz. - 10 kHz.
J	-8	5 kHz.	1kHz. - 10 kHz.
K	-10	5 kHz.	1kHz. - 10 kHz.
L	-5	5 kHz.	2kHz. - 10 kHz.
M	-8	5 kHz.	1kHz. - 10 kHz.
N	-15	5 kHz.	1kHz. - 10 kHz.
O	-7	5 kHz.	3kHz. - 10 kHz.
P	-10	5 kHz.	2kHz. - 10 kHz.
Q	-12	5 kHz.	3kHz. - 10 kHz.
R	-7	5 kHz.	1kHz. - 10 kHz.
S	-10	5 kHz.	1kHz. - 10 kHz.
T	-14	10 kHz.	3kHz. - 10 kHz.

Tables 7 and 8 show that, in general, the TNM is under-predicting at the higher frequency range of 1250 Hz to 10 kHz. for Microphone Position 1. These differences are thought to be the result of refraction effects since this type of deviation is not present in the reference spectrum mentioned earlier. TNM and many other noise prediction models usually ignore refraction effects which are normally present in the higher frequency ranges and this is thought to be a large source of error. Figure 4 shows examples of sites and microphones that had the largest high frequency errors as indicated in Tables 7 and 8. These plots are full spectrum plots and not only indicate the high frequency errors but also show that the low frequency, ground effect errors are very obvious. The following section investigates the correlation between TNM high frequency errors and measured meteorological conditions at each site.

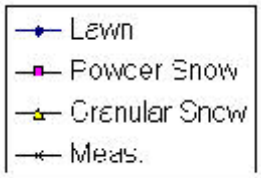

Figure 4. High Frequency Deviations Between Measured and Predicted Sound Levels.

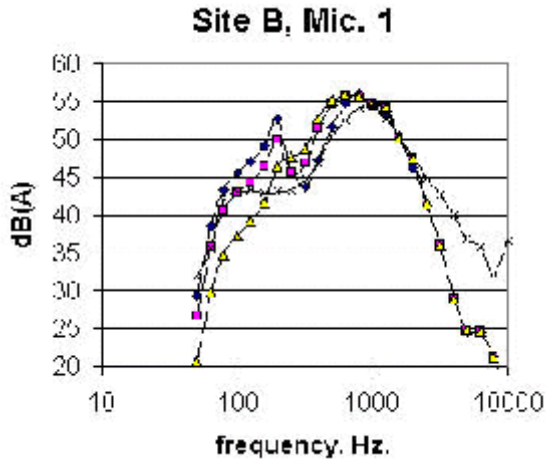

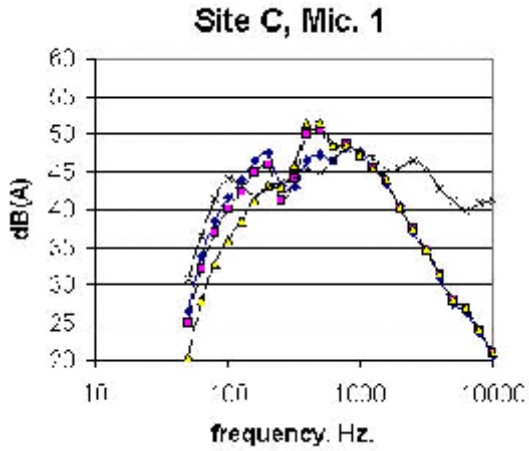

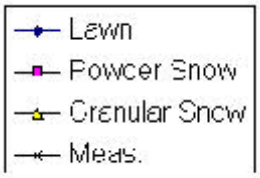

Figure 4. High Frequency Deviations Between Measured and Predicted Sound Levels.

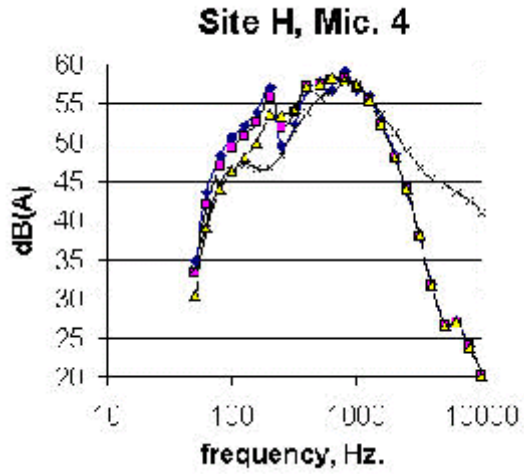

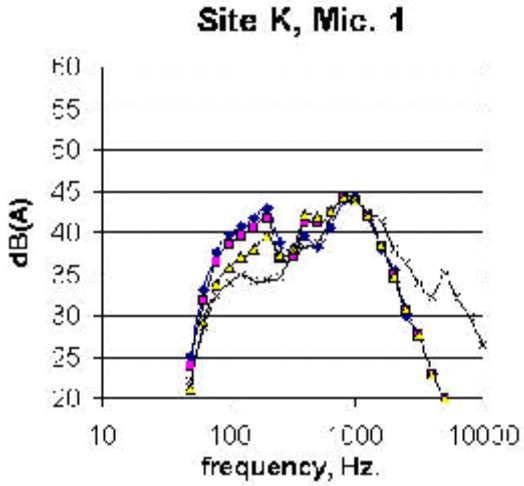

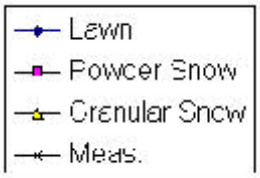

Figure 4. High Frequency Deviations Between Measured and Predicted Sound Levels.

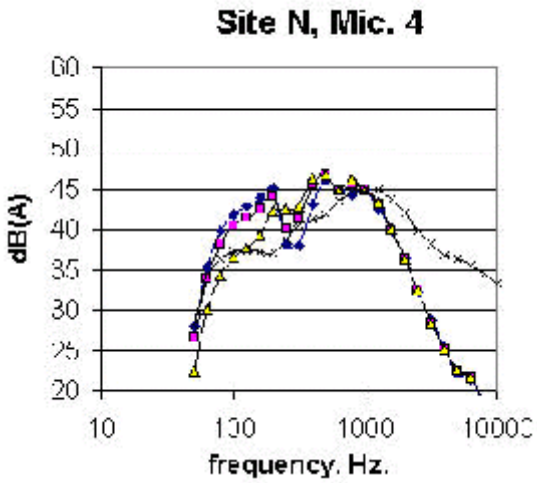

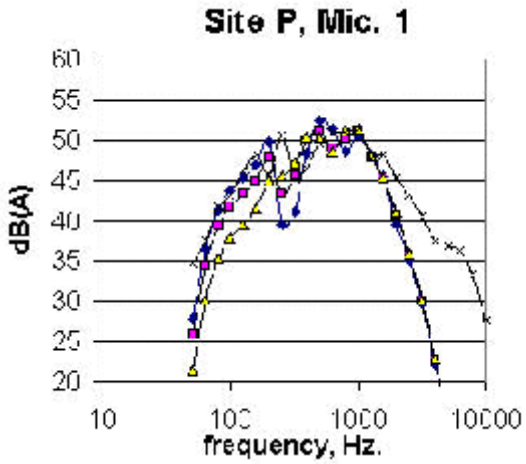

D. Correlation Between TNM Errors and Meteorological Effects

The high frequency TNM prediction errors noted in the previous section were further investigated. The TNM errors at Microphone Locations 1 and 4 were correlated against the measured wind shear (wind

moving from barrier to receiver 'pos' and receiver to barrier 'neg') and lapse rate for all sites to see whether the TNM error is correlates to meteorological effects and therefore to refraction errors. Tables 9, 10, 11, and 12 contain the R^2 results for TNM predictions errors versus measured lapse rate and wind shear. Figure 5 show this graphically.

Table 9. R^2 Results for SPL Errors (Predicted - Measured)

Met. Component	Mic1 error	Mic4 error	Avg. Error
wind, pos	0.02	**0.19**	0.13
wind, neg	**0.17**	0.00	0.01
lapse rate	0.05	0.00	0.00

Table 10. R^2 Results for Propagation Loss Errors (Predicted - Measured)

Met Component	Mic1 error	Mic4 error	Avg. Error
wind, pos	0.00	0.27	0.25
wind, neg	0.04	0.28	0.32
lapse rate	0.02	0.40	0.39

Table 11. R^2 Results for SPL Errors (ABS[Predicted - Measured])

Met Component	Mic1 error	Mic4 error	Avg. Error
wind, pos	0.01	**0.44**	**0.32**
wind, neg	0.06	0.05	0.00
lapse rate	0.03	0.21	0.04

Table 12. R^2 Results for Propagation Loss Errors (ABS [Predicted - Measured])

Met Component	Mic1 error	Mic4 error	Avg. Error
wind, pos	0.01	0.24	0.18
wind, neg	0.01	0.31	0.20
lapse rate	0.01	**0.46**	0.20

Figure 5. TNM Error Versus Lapse Rate and Wind Shear

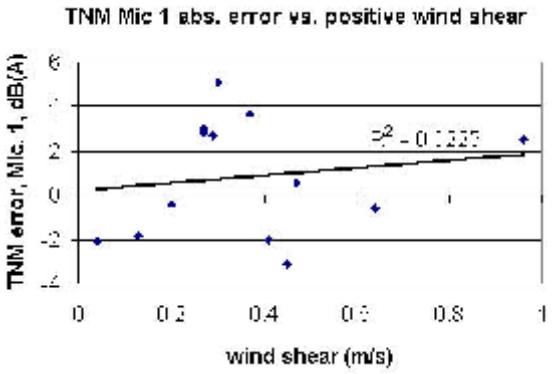

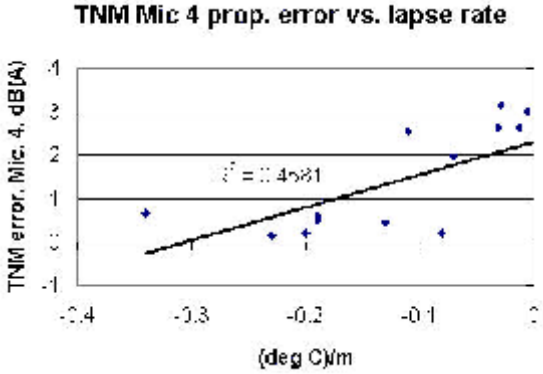

Tables 9 to12 show that there is no obvious, strong correlation between TNM error and meteorological effects. The highest correlation coefficient was 0.46 of the TNM propagation losses for microphone 4 and lapse rate. The highest correlation for sound pressure levels was 0.44 for microphone 4 and positive wind shear. These are not considered to be high correlation coefficients but it does show some correlation, in other words 40-50 % of the variation can be explained by meteorological effects. Since testing was done close to the barrier, and in low wind conditions, low R^2 values could be expected. Figure 5 shows two examples of the range of correlation coefficients shown in Tables 9 to12, the first plot shows the poor correlation between microphone 1 sound levels and wind shear. The second plot

shows better correlation between microphone 4 propagation losses (abs[error]) and lapse rate. This again points to the very low wind speeds as a reason for the lower correlations.

E. TNM Temperature and Humidity Default Values Testing

The Traffic Noise Model (TNM) includes an atmospheric absorption algorithm that uses FHWA recommended default values to compute attenuation of sound pressure over varying distances through the air. The TNM default values for the temperature and relative humidity default to 68/F and 50% respectively. However, the actual weather conditions at the measurement sites usually had much higher values than the default values used in TNM. This section discusses the difference between the TNM predicted sound levels when using the measured temperature and relative humidity for each site, compared to the default values. Table 13 shows the measured parameters at Sites M-T, the sites visited during Part II of this work.

When applying the specific values for each site, TNM predicted sound levels tend to be reduced by 0.1 dB(A) than the originally predicted sound levels when using the FHWA default values. Site M was the only exception, since its temperature and relative humidity were similar to TNM default values. A difference of 0.1 dB(A) is not considered to be significant. Usually, significant reduction in atmospheric absorption is observed at greater distances from the noise source than measured for this research. This explains the small reduction in TNM levels observed in these sites, since the furthest microphones (Microphone Positions 1, 2 and 3) were at a distance of only 30 meter from the noise barrier. Tables 14 and 15 show this reduction for Microphone Positions 1 and 2 specific to each site.

Utilizing the measured values for temperature and relative humidity rather than the default values when predicting sound levels using Traffic Noise Model (TNM) did not result in significant reduction in sound levels due to the small distance between the roadways and the microphones.

Table 13. Measured Weather Conditions for Sites M thru T.

Site	Temperature (/F)	Relative Humidity (%)
Site M	71	48
Site N	82	80
Site O	84	85
Site P	78	47
Site Q	78	34
Site R	85	NA
Site S	89	35
Site T	75	59

Table 14. TNM Sound Levels in (dB) for Microphone Position 1.

Site	TNM (Default value) dB(A)	TNM (Measured value) dB(A)
Site M	No change	No change
Site N	52.2	52.1
Site O	66.0	65.9
Site P	59.4	59.3
Site Q	60.4	60.3
Site R	NA	NA
Site S	54.3	54.2
Site T	71.2	71.1

Table 15. TNM Sound Levels in (dB) for Microphone Position 2.

Site	TNM (Default value) dB(A)	TNM (Measured value) dB(A)
Site M	No change	No change
Site N	53.6	53.5
Site O	67.2	67.1
Site P	61.0	60.9
Site Q	62.2	62.1
Site R	NA	NA
Site S	55.8	55.7
Site T	72.1	72.0

V. VISUALIZATION OF SOUND LEVELS AND SHADOW ZONES

Custom software was developed, as part of this work, to visualize the measured and predicted sound pressure levels and insertion losses behind highway noise barriers. The software includes plotting features for the measured data at the nineteen barrier sites and importing/plotting and interpolation features for TNM predicted sound levels and insertion losses. The TNM models were modified by adding 200-300 receivers behind the barrier to produce a grid of sound pressure level and insertion loss. These results were imported into the custom software package and, together with a developed 'acoustic energy interpolator', the software produces graphical depictions of sound levels and insertion losses that cannot be fully appreciated by a review of numerical results.

Figures 6 and 7 contain the graphical results of this software. Figure 6 shows plots of sound pressure level behind the barrier for each of the nineteen sites while Figure 7 includes a plot of insertion loss for each site. A legend describing the color scheme is also included at the top of each figure. In general, a red color represents a high sound pressure level (80 dB[A] or higher), green represents a low sound pressure level. In terms of insertion loss, red also represents low insertion loss and green represents high insertion loss (15 dB and higher). The different regions of sound pressure and insertion loss are clear to see from these plots and the nature of the barrier diffraction is visible along with interesting effects on insertion loss due to the absorptive ground surface. A brief discussion of each site is also included for clarity.

The plots of sound pressure level shown in Figure 6 have the ability to show immediately the effects that have been discussed in Parts 1 and 2 of this project. A picture is worth a thousand words and these plots show many interesting results. In general, plots with large red regions either correspond to high sound levels from traffic or to poor diffraction by the barrier and knowledge of each site helps to draw the following conclusions.

Site A: This site had a tall barrier and the large amount of green color in the plot indicates good shielding by the barrier.

Site B: This site was similar in location and geometry to Site A and has a similar diffraction pattern but it is evident that the smaller effective wall height leads to a diminished shadow zone, compared to Site A.

Site C: There is good shielding by the wall and a nice shadow zone.

Site E: This site had a large berm and a six foot barrier. The berm outline is noticeable in the plot. The berm/barrier combination is providing good shielding.

Site F: This barrier is not as tall as the previous sites but still shows a nice green area behind the wall and a good shadow zone

Figure 6. Sound Pressure Level Plots (from TNM results)

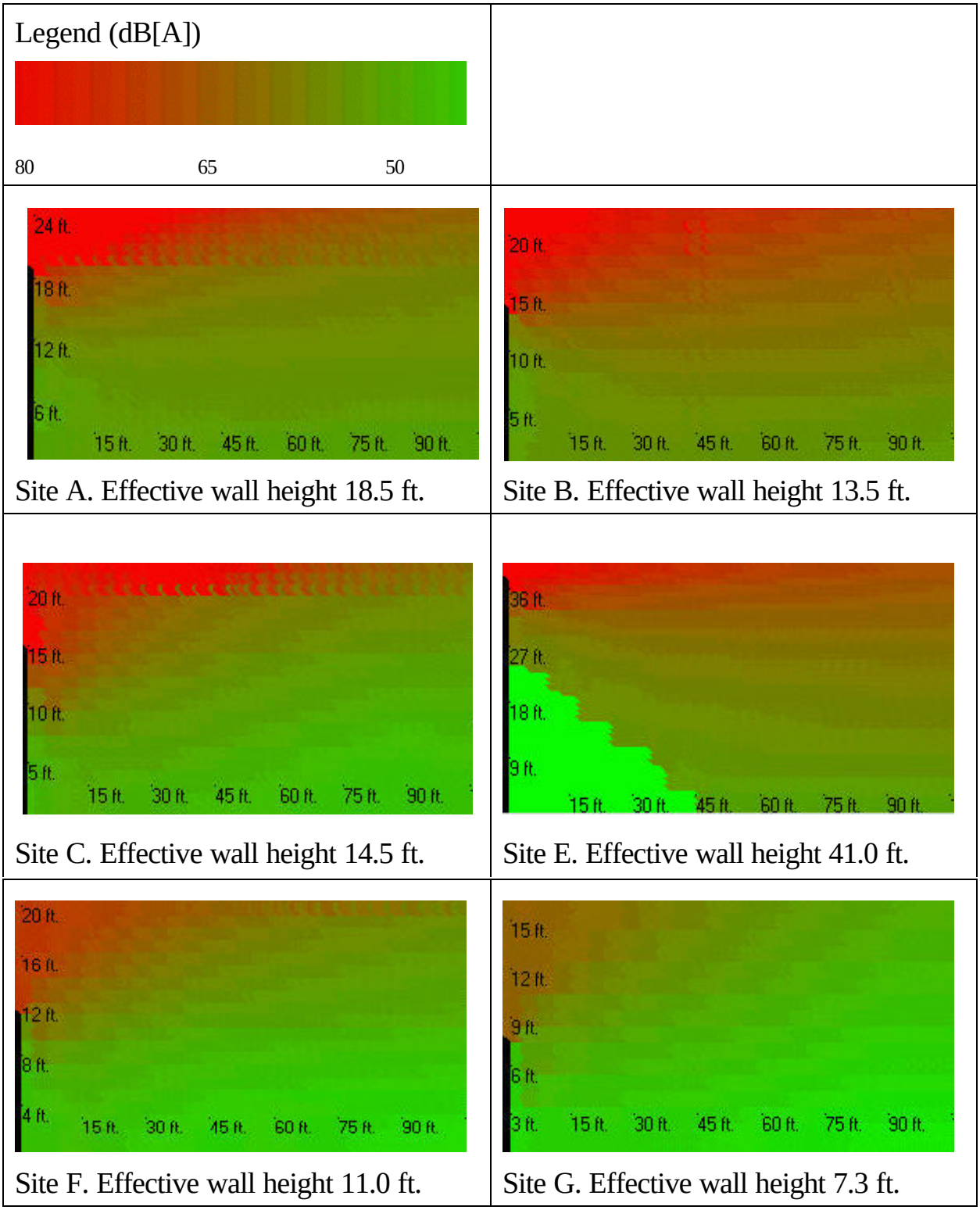

Site A. Effective wall height 18.5 ft.

Site B. Effective wall height 13.5 ft.

Site C. Effective wall height 14.5 ft.

Site E. Effective wall height 41.0 ft.

Site F. Effective wall height 11.0 ft.

Site G. Effective wall height 7.3 ft.

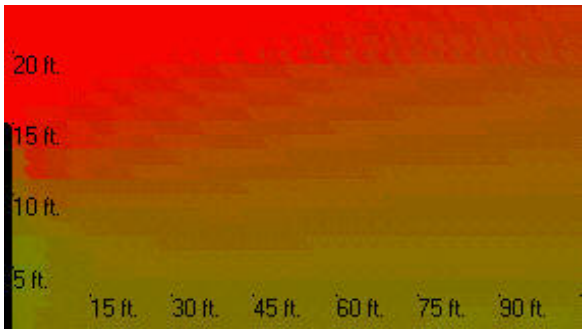

Site H. Effective wall height 14.5 ft.

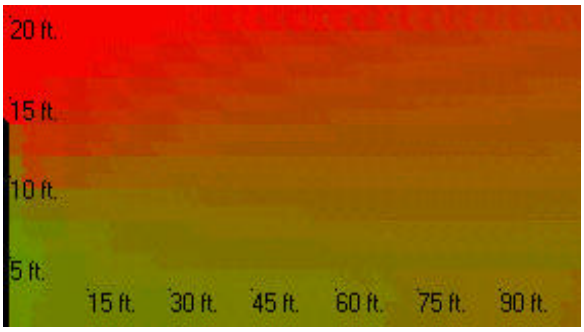

Site I. Effective wall height 13.1 ft.

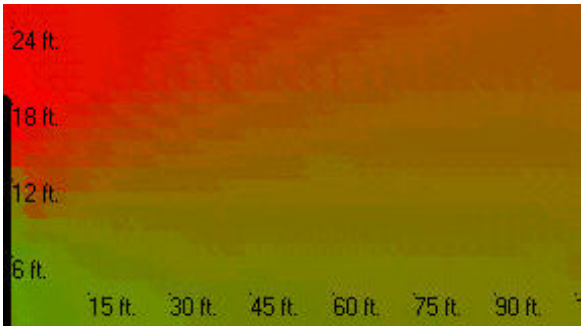

Site J. Effective wall height 18 ft.

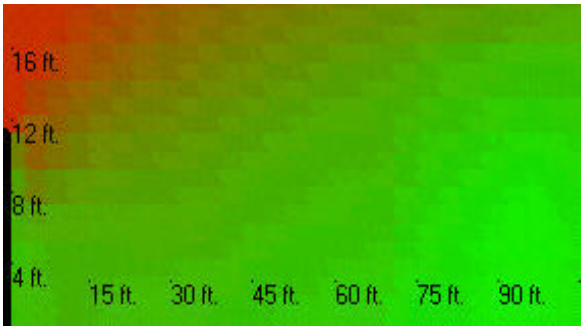

Site K. Effective wall height 11.0 ft.

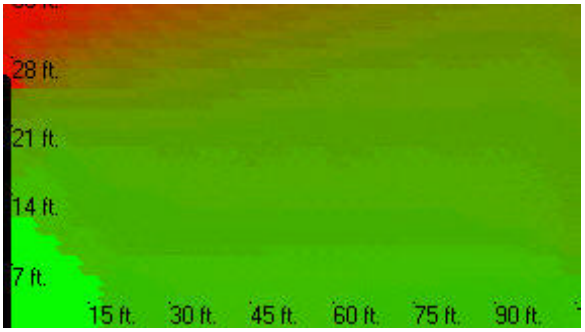

Site L. Effective wall height 25.3 ft.

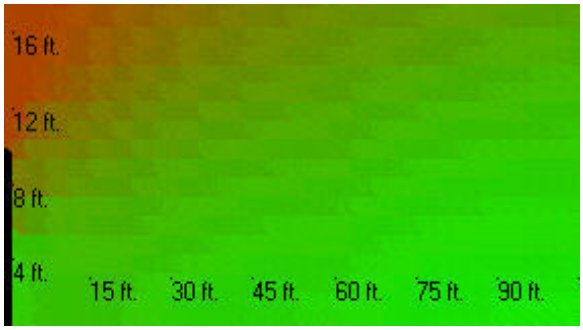

Site M. Effective wall height 9.4 ft.

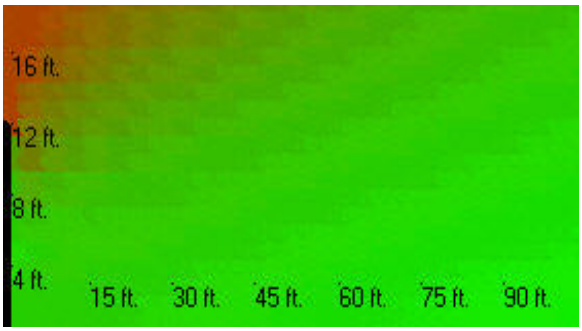

Site N. Effective wall height 11.6 ft.

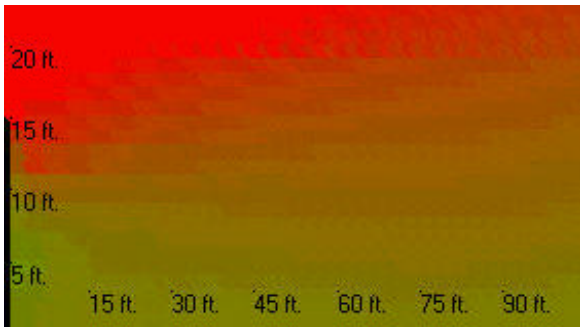

Site O. Effective wall height 14.5 ft.

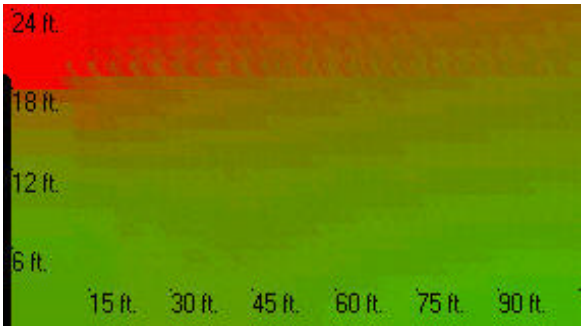

Site P. Effective wall height 18.4 ft.

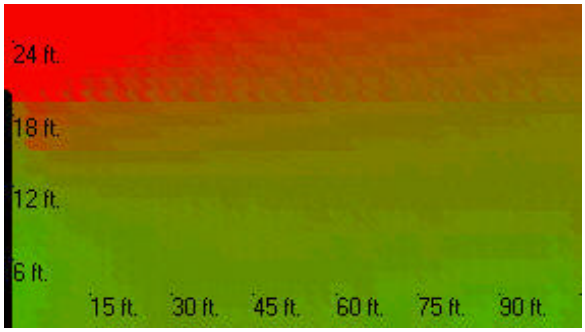

Site Q. Effective wall height 19.3 ft.

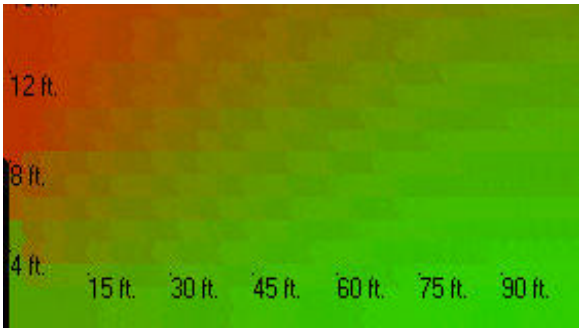

Site R. Effective wall height 7.7 ft.

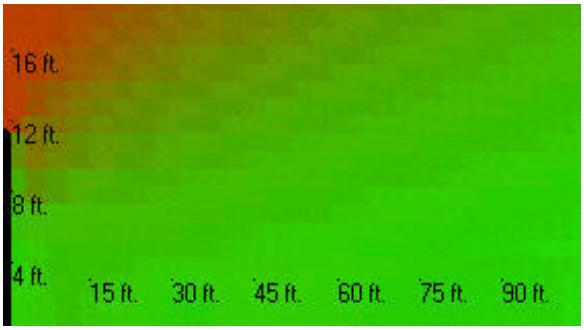

Site S. Effective wall height 11 ft.

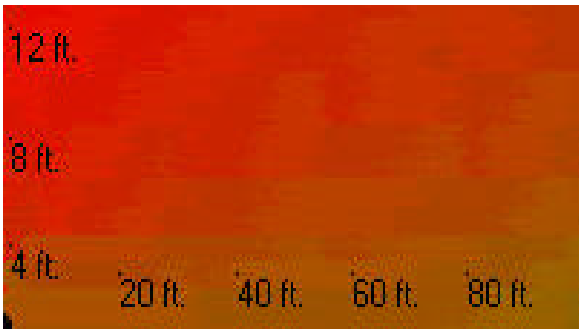

Site T. Effective wall height 0.0 ft.

Figure 7. Insertion Loss Plots (from TNM results)

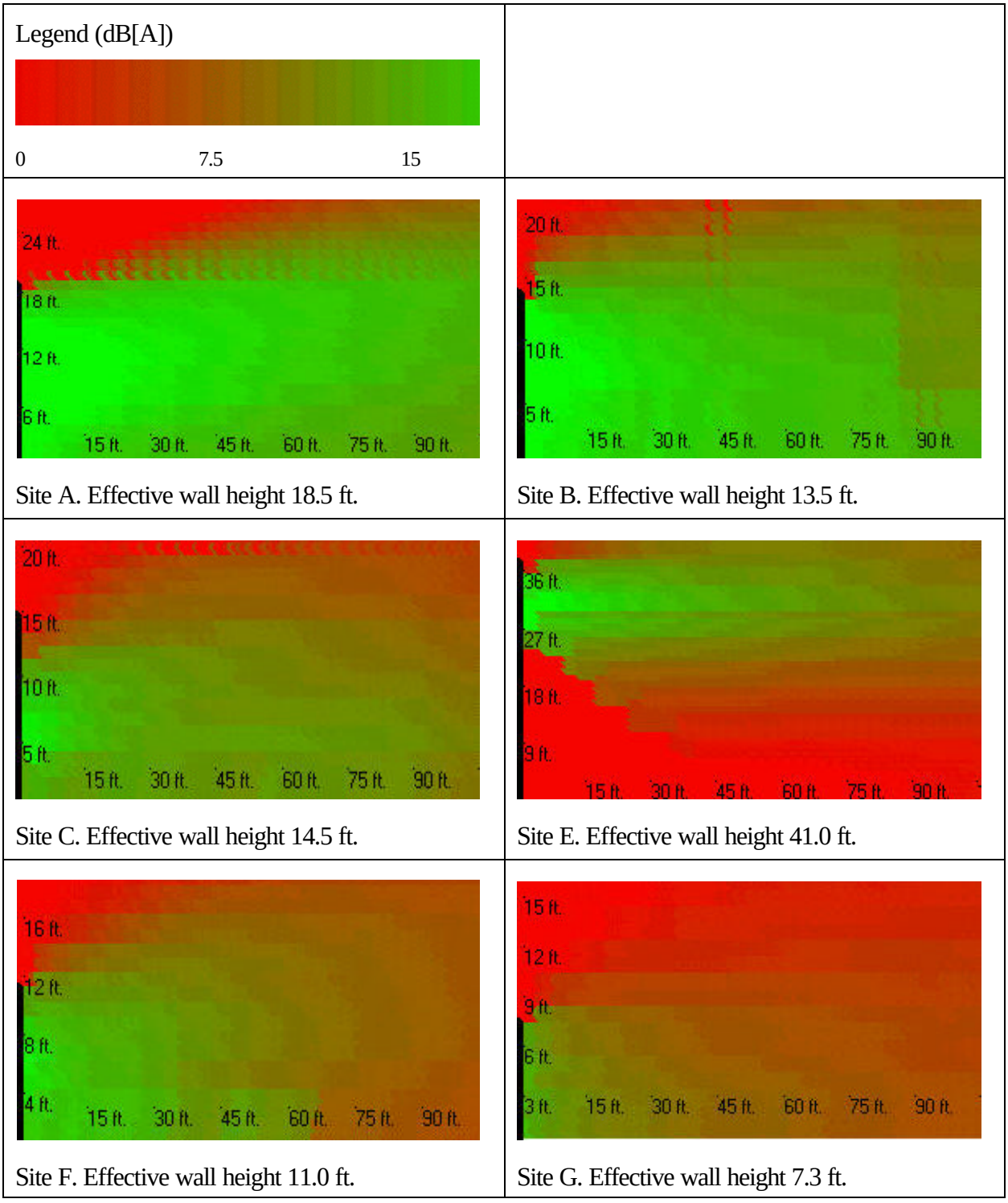

Site A. Effective wall height 18.5 ft.

Site B. Effective wall height 13.5 ft.

Site C. Effective wall height 14.5 ft.

Site E. Effective wall height 41.0 ft.

Site F. Effective wall height 11.0 ft.

Site G. Effective wall height 7.3 ft.

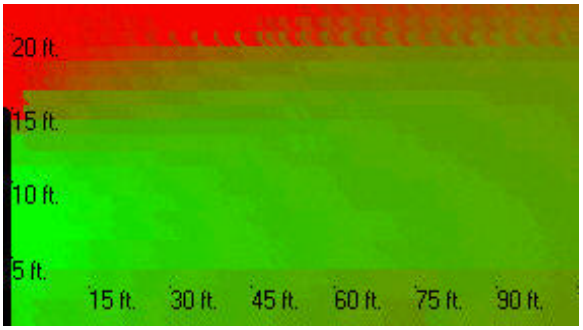

Site H. Effective wall height 14.5 ft.

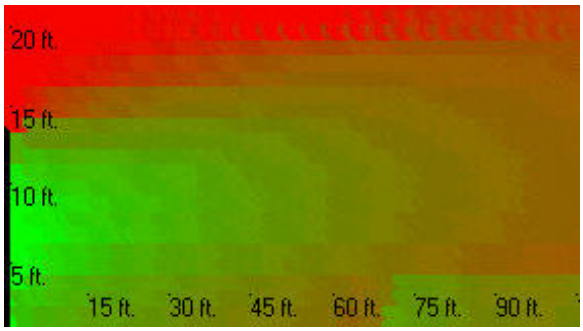

Site I. Effective wall height 13.1 ft.

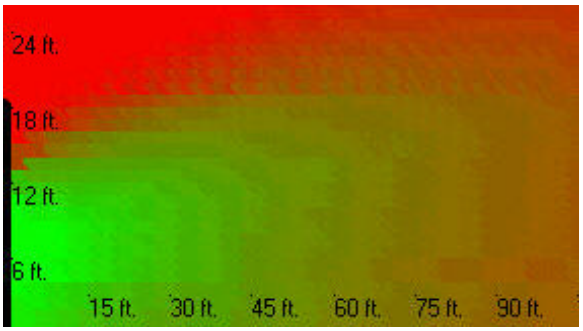

Site J. Effective wall height 18 ft.

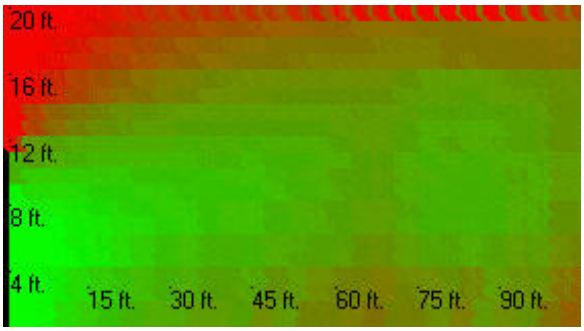

Site K. Effective wall height 11.0 ft.

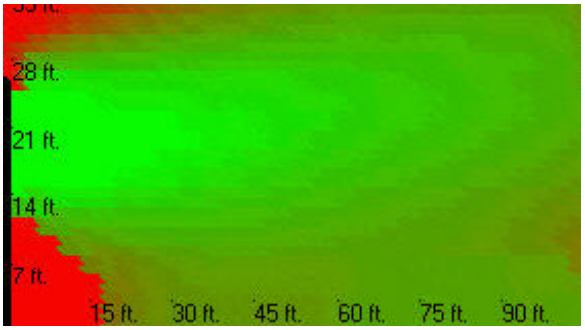

Site L. Effective wall height 25.3 ft.

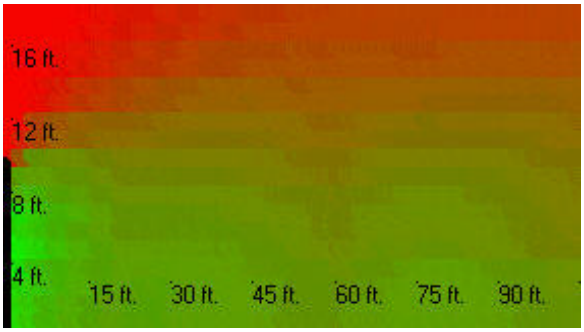

Site M. Effective wall height 9.4 ft.

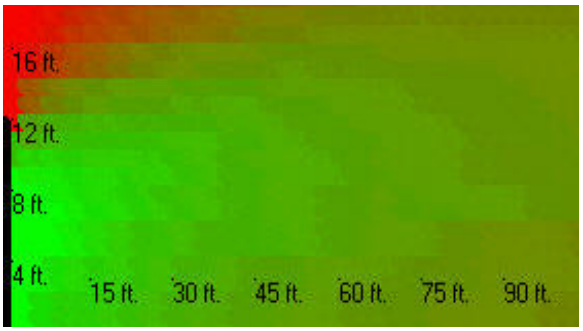

Site N. Effective wall height 11.6 ft.

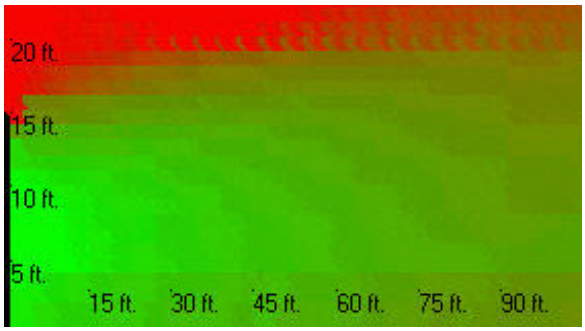

Site O. Effective wall height 14.5 ft.

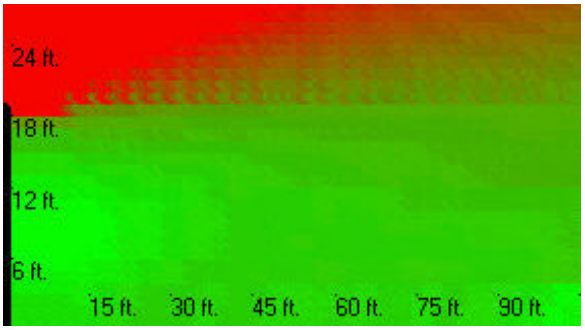

Site P. Effective wall height 18.4 ft.

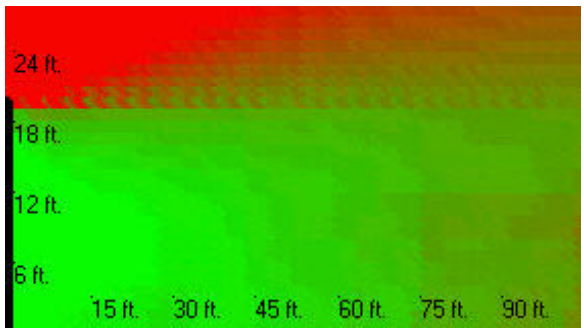

Site Q. Effective wall height 19.3 ft.

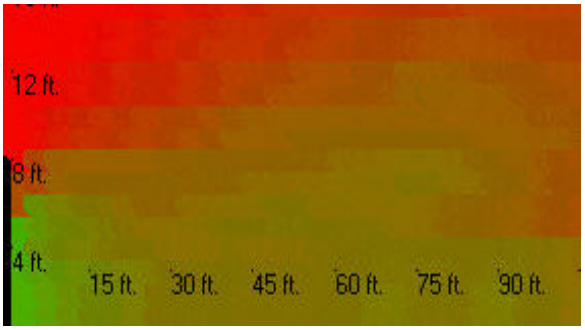

Site R. Effective wall height 7.7 ft.

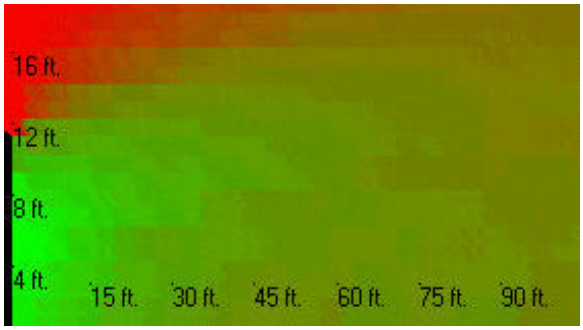

Site S. Effective wall height 11 ft.

Site T. Effective wall height 0.0 ft. resulting in no insertion loss

Site G: This barrier is the shortest that we tested. The green color behind the wall is more a function of the low source levels than the wall effectiveness.

Sites H and I: These plots indicate large amounts of red area due to the high source levels from Interstate 95 and the fact that the barriers were somewhat ineffectual due to their height.

Site J: This is another site with a berm/barrier combination but we see that even with a wall height of 18 feet, the shadow zone is degraded and not as green as other plots in the table. One of the major reasons for this is that there was a roadway behind the barrier which was an on-ramp onto the highway. This introduced a strong background source that degraded the shadow zone.

Site K: This site did not have a large wall but the large green areas show that it was effective in shielding the source. Also, the source was not a highway but an interrupted flow roadway with lower source levels than a highway.

Site L: This is another berm/barrier combination but its much more effective than Site J due to its larger size and absence of an intrusive background source.

Site M: This site had a relatively short wall and sporadic traffic and shows good shielding and shadow zone.

Site N: This plot is nearly all green, indicating good shielding and shadow zone, the source levels in this case were not very high.

Site O: This site is a repeat of Site H and shows very similar results, as expected, poor shadow zone and shielding due to the high source strength and wall height.

Site P: This is a large barrier along I95 and the plot shows that to effectively shield I95 it requires more than 14-15 feet. This wall is providing a good shadow zone.

Site Q: This is another barrier along I95 and even though its taller than site P, it appears to be less effective, this may be due to refractive effects.

Site R: This is a low barrier but it is on elevated ground, not necessarily a berm, and because of this provides a good shadow zone.

Site S: This barrier is providing a good shadow zone for this site and is effective with the sources on the shielded roadway.

Site T: This is the most dramatic example of large red areas due to no barrier. This results in high sound pressure levels beyond the I-4 right of way with some reduction close to the ground.

VI. INSERTION LOSS DISCUSSION

Insertion loss is the result of placement of a barrier between a source and a receiver, resulting in a reduction of sound levels at the receiver. Insertion loss from highway noise barriers is a function of barrier attenuation, shielding, ground effects, transmission loss through the barrier, reflections, and flanking noise. Refraction effects may also affect insertion loss as changes in weather occur. Insertion loss (IL) is determined by Equation (6).

$$IL = SPL_{before} - SPL_{after} \quad (6)$$

Figure 7 shows graphs of TNM predicted insertion loss behind each of the barriers studied. These plots permit the researchers to visualize the insertion losses, how they extend behind the noise barriers, and the influence of ground effects In many cases, insertion loss near the top of the wall and close to the ground is low (indicated by a red color), with a bright green section of higher insertion loss 'sandwiched' between them. This effect occurs since sound levels high above the ground are not benefitted by barrier diffraction and sound levels near the ground have had beneficial ground effects removed by the placement of the barrier. The following is a brief summary of insertion loss trends for each site.

Site A: This site had a tall barrier and the large amount of green color in the plot indicates good insertion loss by the barrier.

Site B: This site has similar results to Site A, good insertion loss behind the barrier and a minimum of degraded insertion loss due to ground effects.

Site C: There is good shielding behind the wall but we can start to see degradation of the shadow zone at 100 ft.

Site E: This site had a large berm and a six foot barrier. The berm outline is noticeable in the plot as the bright red region directly behind the wall. This plot shows the effects of removing beneficial ground effects by placing a barrier in the path. There is green 'sandwich' high above the ground plane. This indicates the true shadow of the wall contribution and shows that ground level receivers do not benefit from the wall, their benefit comes almost exclusively from the berm itself.

Site F: The sound pressure plot for this site showed a nice green area behind the wall indicating low sound levels but the insertion loss plot shows that the wall benefit is only extending out to about 90 feet. This indicates that the low sound levels were due to a low source strength.

Site G: This barrier is the shortest that we tested and once again the insertion loss plot provides more information about the barrier effectiveness than the sound level plot. The sound levels behind the

barrier were low and desirable but the insertion loss plot shows that this wall is providing minimal shielding.

Sites H: The insertion loss plot shows good shielding from Interstate 95 and indicates that the unfavorable sound level plots were a result of elevated source levels and not ineffective barrier design.

Site I: This insertion loss plot does show degradation of the shadow within 90 feet and supports the sound level plot that the barrier is marginally effective.

Site J: This site had the busy on-ramp behind the barrier and we can see this effect by the encroachment of background sound shown in the insertion loss plot.

Site K: This plot shows good insertion loss at this site and indicates an effective barrier design for the site conditions.

Site L: This is another berm/barrier combination but its much more effective than Site E as evidenced by the large green area behind the barrier. Some reduced insertion loss is shown near the ground but overall the design is effective.

Site M: This site had a relatively short wall and the insertion loss plot shows that it is effective.

Site N: This plot is nearly all green as was the sound level plot. This indicates good shielding and shadow zone.

Site O: This site is a repeat of Site H and shows very similar results to the site H insertion loss plot, good shielding, which contradicts the sound level plot and points to a strong source rather than an ineffective barrier.

Site P: This is a large barrier along Interstate 95 and the plot shows good protection by the barrier.

Site Q: This is another barrier along Interstate 95 and even though its taller than site P, it appears to be less effective, this may be due to refractive effects. These results are similar to conclusions drawn from the sound level plots.

Site R: This is a low barrier but it is on elevated ground, the sound level plot showed favorable results but the insertion loss plot shows that the barrier is marginally effective and that most of the shielding is due to the elevated ground at the barrier.

Site S: This barrier is providing a good shadow zone for this site and is effective with the sources on the shielded roadway.

Site T: This site does not have a barrier. Insertion loss is zero and accordingly, not plotted.

Overall, the numerical results and the graphics showed that barriers tested in Florida were effective and provided protection out to the second row of homes with some exceptions due to line of sight issues (Sites G and R) and edge effects (Site F).

VII. SHADOW ZONE LENGTH ESTIMATION

Insertion loss can be used to determine the edge of the shadow zone by predicting where the insertion loss is zero. This was the method used in the previous report [2] to determine the edge of the shadow zone. That method required TNM results to estimate the length of shadow zone which introduces some inconvenience for a DOT planner. A more desirable method would be one that does not require results from a sophisticated computer model of the proposed site.

The previous report [2] described two regression equations to predict shadow zone length behind a barrier. Both models require TNM predicted sound levels behind the modeled barrier. Equation (7) is the regression equation developed for ANSI corrected TNM predicted insertion loss. To use this method, first the TNM insertion loss must be determined by building a TNM model and then this value must be adjusted with an error estimate based on actual sound level measurements at the site. Equation (7) had a goodness of fit R^2 value of 0.71 out of a maximum value of one.

$$SZL = 53.15 \exp (0.195 * IL_{30}) \quad (7)$$

where: SZL = shadow zone length, ft.
IL_{30} = the ANSI corrected insertion loss, 98.4 ft. (30 meters) behind the barrier

Equation (8) can be used to predict shadow zone length from the uncorrected TNM predicted insertion loss. This means that no additional information is required from the site other than geometric information to build a model. This equation had an R^2 value of 0.40 out of a maximum value of one.

$$SZL = 52.2 \exp (0.17 IL_{TNM}) \quad (8)$$

where: IL_{TNM} = Insertion loss predicted by TNM at 98.4 feet (30 meters) behind the barrier

These methods provided some value in determining the edge of the shadow zone but were cumbersome

since they required TNM results and possibly field measurements. A better, single equation, method was sought that did not require computer model results or detailed sound level data from the proposed site. To accomplish this, the measured sound level data from all sites was used to construct an empirical relationship of the sound pressure level 'delta' behind a barrier versus parameters such as distance from the barrier, height of the barrier and height of the receiver. This 'delta' value is the difference between the reference level (above the wall) and the sound level at a position behind the barrier. Equation 9 was developed using the data collected during this project. The regression equation was generated using 155 data points and resulted in a 0.79 R^2 value.

$$\Delta_{spl} = 24.7 + 0.03 * dist - 0.35 * ht + 0.34 * wall - 0.27 * L90 + 0.02 * road - 16.2 * HT \quad (9)$$

where: ? $_{spl}$ = reference sound level - sound level behind the wall
dist = distance from wall to receiver, ft.
ht = height of receiver above ground, ft.
wall = height of wall, ft.
L_{90} = background sound level of location, dB(A)
road = distance from wall to roadway centerline, ft.
HT = fraction of heavy trucks operating on roadway (0-1.0)

Equation 9 can be used to estimate sound levels behind a theoretical sound barrier and also to estimate the shadow zone length by finding the distance behind the barrier where the sound pressure level reaches the background (L_{90}) level. Equation 10 can be used when L_{99} is the known or desired background level. Although this method does not require TNM results it does require an estimate of L_{Aeq} reference sound level due to the roadway and estimated background sound levels for the site. This will require either measurements or modeling a site 5 feet above the barrier wall location using TNM.

$$\Delta_{spl} = 22.2 + 0.03 * dist - 0.35 * ht + 0.31 * wall - 0.22 * L99 + 0.02 * road - 14.7 * HT \quad (10)$$

where: ? $_{spl}$ = reference sound level - sound level behind the wall
dist = distance from wall to receiver, ft.
ht = height of receiver above ground, ft.
wall = height of wall, ft.
L_{99} = background sound level of location, dB(A)
road = distance from wall to roadway centerline, ft.
HT = fraction of heavy trucks operating on roadway (0-1.0)

Table 16 contains the average error (compared to the measured sound levels) of Equation 9 using the regression technique for each site and microphone. Table 16 shows that the average error for all microphone positions and all sites, using the regression equation, is -1.2 dB(A). The average residual error (absolute error) is 2.2 dB(A). This gives an indication of the error expected when using the regression equation in the range of 100 feet beyond a barrier and up to 20 feet off the ground. This was considered quite acceptable.

Table 16. Site Average Residual Error of Regression Method at Each Site (Microphone Positions 1 thru 8, A, C, No Rovers; Error = Predicted SPL-Measured SPL).

Site	avg. abs(error), dB(A)	avg. error, dB(A)
A	1.4	-0.4
B	1.9	-1.9
C	2.1	-2.1
E	2.3	-2.0
F	2.3	-2.3
G	1.7	-1.2
H	1.7	-0.2
I	1.8	-1.8
J	1.6	-0.1
K	2.9	0.3
L	2.1	-1.5
M	2.6	-0.4
N	2.2	-1.4
O	2.6	0.2
P	1.7	-0.8
Q	2.0	-0.6
R	4.4	-4.1
S	2.4	-2.1
T	1.8	0.1
avg.	2.2	-1.2
stdev	0.7	1.1

The presented regression method for determination of sound pressure level behind a barrier (Equations 9 and 10) and is based on measurements from the 19 Florida barrier sites. The regression method is valid for receiver locations at distances up to 30 meters from the barrier 6 meters above the ground

plane (except for Rover results which were beyond 30 meters). At distances greater than 30 meters, the regression equation predicts decreasing sound levels as distance from the barrier increases. Equations 9 and 10 will predict a steady decrease in sound level as distance from the barrier increases, even though the sound level eventually reaches a background level and stabilizes. The method has no mechanism to counter this decreasing effect since it is based primarily on measurements within 30 meters of the barrier, well within the shadow zone in most cases.

To further develop this idea for greater distances, a background source contribution was developed that introduces a point source into the environment to act as the 'virtual' background source. Background sound level is not a feature of most traffic noise models and for this reason they predict theoretical shadow zones that extend further than actually occurs in practice.

The rover measurements were then used to develop and evaluate a method of locating the position and strength of a generic background source to be included in the method. Table 17 is a summary of the average error of rover sound level prediction using the regression Equation 9 with the background source feature included. Table 17 shows that the error of predicting the rover sound levels with the regression equation only, was 4.8 dB(A), which is considered to be high. With the introduction of the background source method this prediction error dropped to 1.1 dB(A), a marked improvement.

Table 17. Rover Error Results With Background Source Feature.

Method	**error, dB(A)**
regress only	4.8
Regress with background	1.1
n	15

This reduction in error are only for the rover microphones which are at greater distances and does not apply at the previously defined microphone postions (1-8, A, C). Table 18 summarizes the error between these two methods when all microphone positions are included. Table 18 shows that, in this case, the error improvement from the regression method only to the regression method with the background source feature was 2.4 to 2.0 dB(A). This is a minor improvement. As such, it cannot be stated that the background source inclusion would improve the average error if microphone positions, including those at greater distances were included.

Table 18. All Microphone Error Results With Background Source Feature.

Method	error, dB(A)
regress only	2.4
Regress with background	2.0
n	172

The shadow zone length prediction method was modified, based on the results of Tables 17 and 18, to include the 'virtual' background source. Table 19 summarizes the shadow zone length estimates using all methods developed by this work. This includes the TNM adjusted IL method (Equation 7), TNM IL method (Equation 8), new regression method (Equations 9 and 10) and the regression method with the background source inclusion. The last column of Table 19 is the estimated length of shadow zone based on rover microphone results. Figure 8 is a plot of the results of Table 19.

Table 19. Shadow Zone Length Predictions and Measurements, ft.

Site	regress only	regress w/BG	TNM/ ANSI	TNM IL	Rover est.
A	113	136	198	271	--
B	148	177	140	229	--
C	194	256	287	184	--
E	105	134	255	258	--
F	227	243	94	126	--
G	130	194	87	99	--
H	180	208	271	276	--
I	144	170	139	140	--
J	132	154	134	174	--
K	345	263	202	249	--
L	148	330	198	253	--
M	449	238	265	183	--
N	256	228	124	221	200
O	234	280	298	281	240
P	197	296	377	422	--
Q	218	278	293	210	320
R	261	217	218	249	230
S	141	235	198	210	--
T	--	--		--	--

The results of Table 19 were used to generate a regression equation of shadow zone length versus important site parameters. Equation 11 can be used to estimate the length of the shadow zone (R^2 = 0.701) in feet, given barrier height, background level, distance to the roadway and the fraction of heavy trucks on the roadway.

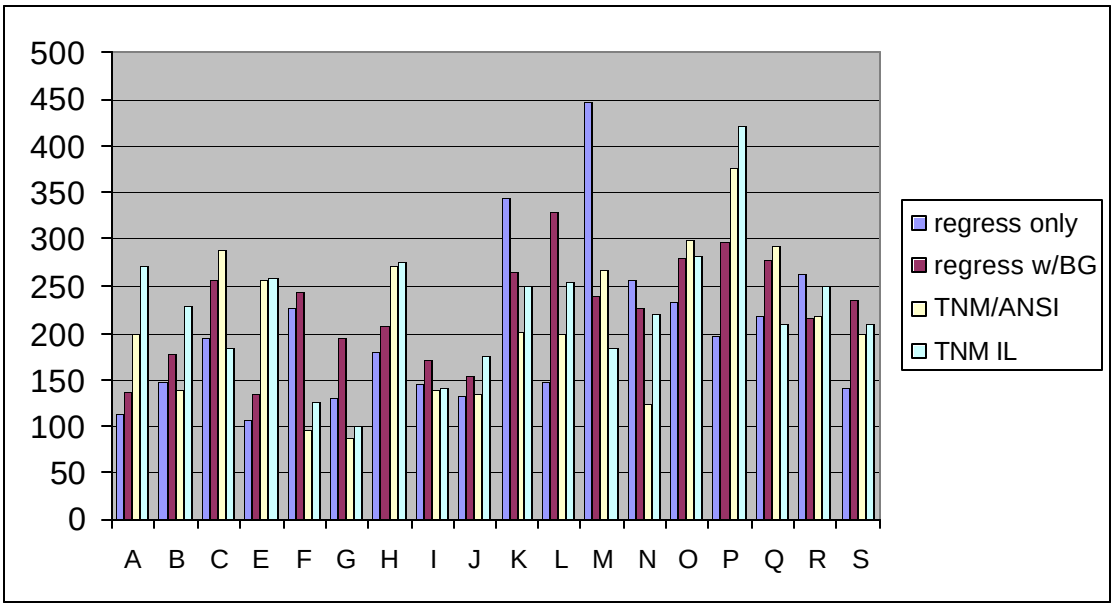

Figure 8. Shadow Zone Length Predictions for All Sites, Using Four Methods.

$$SZL = 616.5 + 2.17 * wall - 9.56 * L90 + 1.27 * road - 530.46 * HT \quad (11)$$

where: SZL = shadow zone length behind barrier, ft.
wall = height of wall, ft.
L_{90} = background sound level of location, dB(A)
road = distance from wall to roadway centerline, ft.
HT = fraction of heavy trucks operating on roadway (0-1.0)

Equation 11 has some interesting features, including the fact that the parameters, receiver height and

distance from wall are not included as they were in Equations 7 through10. This is expected since you would expect the shadow zone length to be primarily dependent on barrier height, the amount of heavy trucks on the roadway, and the background source strength.

Table 19 and Figure 8 show results using four methods to determine the length of the shadow zone. A description of these methods is the following:

1. **Regress only**: use Equation 9 to estimate location where sound level behind barrier is equal to L_{90} background level

2. **Regress with background**: based on superposition of regression Equation 11 and contribution of 'virtual' background source described in previous section. Use regression Equation 11.

3.**TNM ANSI adjusted IL method**: based on TNM method to model the proposed/existing barrier location and estimate location behind the wall where insertion loss becomes negligible (zero) using the ANSI adjustment from actual measurements (adjusts for TNM prediction error, Equation 7).

4. **TNM raw IL method**: based on TNM method model the proposed/existing barrier location and estimate location behind the wall where raw TNM insertion loss becomes negligible (zero). There is no adjustment in this method for prediction error. Use regression Equation 8.

Table 20 and Figure 9 show that the regression with background source method had the lowest average error in terms of shadow zone length (compared to conclusions drawn from rover measurements). Interestingly, it was found that the regression method with background source had some large L_{90} prediction errors at sites K,M,N and R, 6, 10, 5, 5 dB, respectively. These errors are very similar to observed differences between 'edge of shadow zone' levels and L_{90} levels. In several cases there was a difference of 5 dB(A) between site L_{90} levels and what appeared to be the edge of the barrier shadow zone. This new method (Equation 11) has no requirement of highway source levels or TNM results as did the other methods and therefore provides a useful, single equation, tool for the DOT planner. However, a background level must be measured or assumed.

Table 20. Average Error of Each Shadow Zone Length Method.

Method	**avg. error, ft.**
regress only	49
regress w/BG	31
TNM/ANSI	43
TNM. IL	48

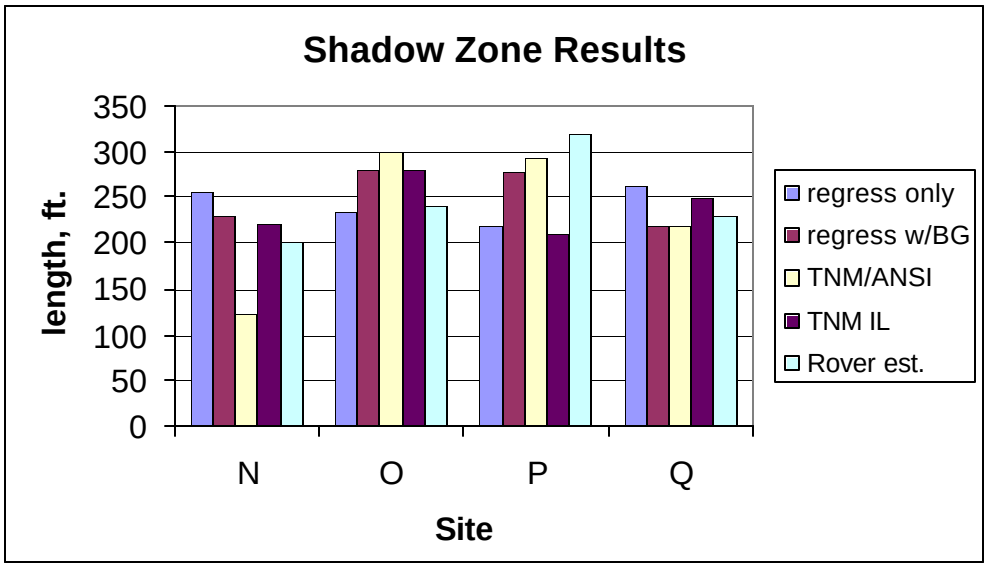

Figure 9.Summary of Shadow Zone Length Predictions Versus Rover Estimates.

A custom software package was also developed during this project to develop and test different shadow zone methods via graphical techniques. This package will be delivered to FDOT for use in highway barrier design. The software imports TNM results from a user-generated comma delimited file and plots the results using an energy interpolator to provide a smooth transition between data points. Once the TNM data is imported, the AutoSZL uses the regression equations previously mentioned to duplicate the site conditions and calculate the regression values on a grid behind the barrier. Both the TNM results and the regression results are then plotted for the user as shown in Figure 10.

Figure 10 shows the TNM results from Site B in the upper plot and the regression equation results in the lower plot. Each plot contains a horizontal and vertical scale and a graphical depiction of the barrier on the left side of the plot (vertical black line). Both plots contains additional black circles which are the locations of the original measured data for each site. The color within the black circles is an indicator of the actual measured sound level. This can be used to visually identify the error between the TNM predicted sound levels and the measured sound levels by looking at the color within the circles and comparing it to the surrounding colors. For example the reference level (Microphone Position 8) in the lower plot is a brighter red than its surroundings, indicating that the regression method is under-predicting sound levels directly above the wall.

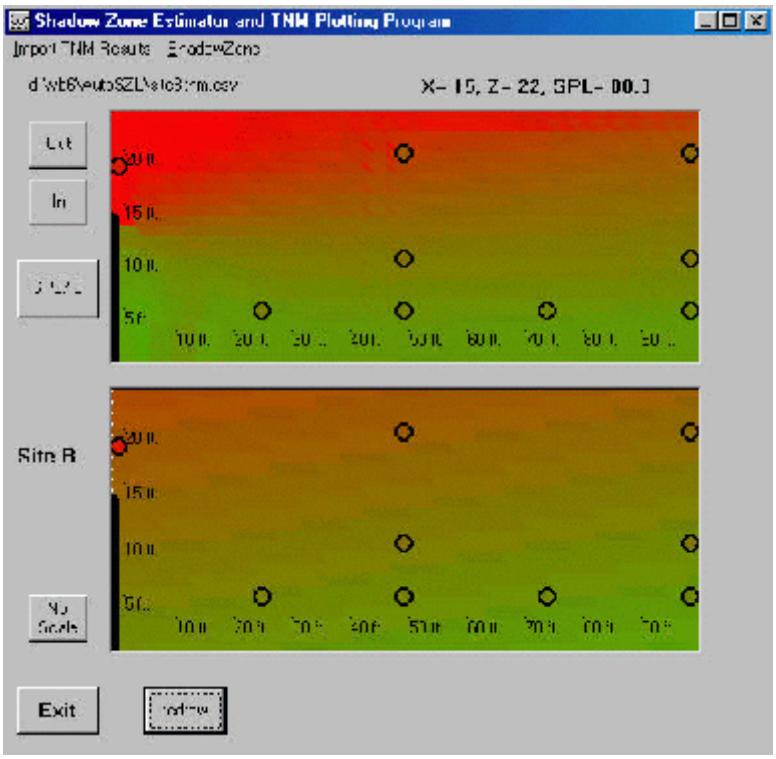

Figure 10.User Interface of AutoSZL Software.

Selecting the ShadowZone menu option shown in Figure 10 starts the Shadow zone length Estimator feature of AutoSZL. This input dialog accepts user input for reference sound level at the barrier, barrier height, background level, distance to shielded roadway and heavy truck information. The AutoSZL computes the shadow zone length based on this information and an iterative scheme that searches for the end of the shadow zone. The empirical regression method of Equation 11 can also be accessed from this input dialog.

VIII. CONCLUSIONS

This work has provided an in-depth look at the effectiveness of the noise barriers in Florida. It has allowed a closer look at the modeling process and has developed software to visualize and estimate shadow zones behind barriers. Important results of this work include the following:

- A new empirical method of predicting shadow zone length behind barriers was developed and requires information readily available to a DOT planner. This method provides a convenient

way to estimate shadow zone length based on actual measurements that include background sound level contribution.

- A new method of background source allocation was developed and used in development of the shadow zone length model.
- TNM predicted reference spectra, above the barrier) were similar to measured spectra.
- An average error of 1 dB(A) was observed in the TNM predicted 'ground dip' but the source of the error is unclear but thought to be due to the angle of the sound wave and the ground plane. A value of about 10 cgs Rayls provided a better fit with measured results than did the default 'lawn' ground type (300 cgs Rayls).
- High frequency effects, caused by refraction (meteorological effects) are not considered in most traffic noise prediction models and this leads to differences between predicted and measured high frequency spectra. However, the effects are small and would seem not to be a primary concern for calm winds and short distances at this time.
- Software was developed to allow visualization of the soundscape and shadow zone behind barriers. This software is being provided to FDOT for use in design of highway noise barriers in Florida.

IX. REFERENCES

[1] Wayson, R., J. MacDonald, W. Arner, P. Tom, D.S.R.K. Srinivas, B. Kim, *Barrier Effectiveness Validation*, Florida Department of Transportation, 2001.

[2] Wayson R., MacDonald J.,et. al., *Continued Evaluation of Noise Barriers in Florida*, FL-ER-85-02, Florida Department of Transportation, 2002.

[3] Lee, C.S.Y. and G.G. Fleming, *Measurement of Highway Related Noise*, FHWA-PD-96-046, U.S. Department of Transportation, Federal Highway Administration, John A. Volpe National Transportation Center, Cambridge, MA, 1996.

[4] American National Standards Institute, *Methods for Determination of Insertion Loss of Outdoor Noise Barriers*, ANSI S12.8-1998, New York, 1998.

[5] International Organization for Standardization, *In-situ determination of insertion loss of outdoor noise barriers of all types*, ISO 10847:1997(E), Geneva, 1997.

[6] Florida Dept. of Transportation, *Project Development and Environment Manual*, Chapter 17, Tallahassee, last updated November 20, 2001.

[7] Delany, M.E., Bazley, E. N., "Monopole radiation in the presence of an absorbing plane." *Journal of Sound and Vibration*, vol. 13(3), pp. 269-279, 1970.

Appendix A

Ground Dip Plots for All Sites (Microphone Positions 1 and 4)

Ground Dip Plots for all Sites: Microphone Position 1

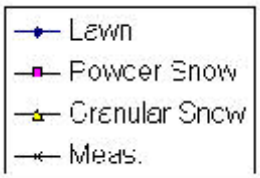

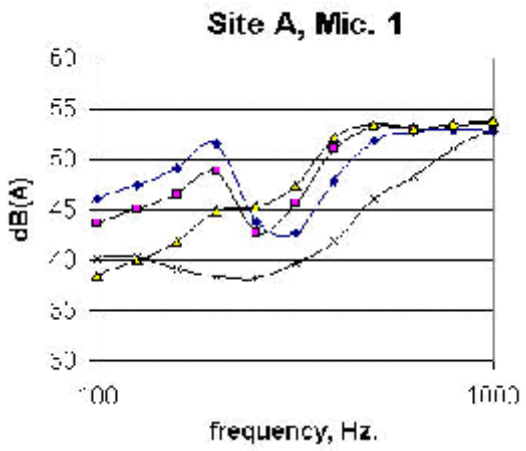

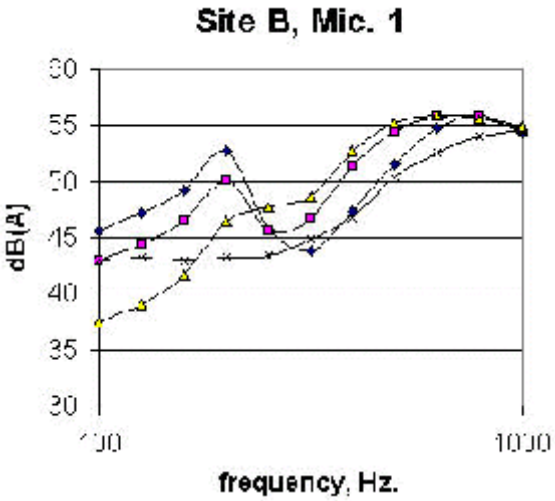

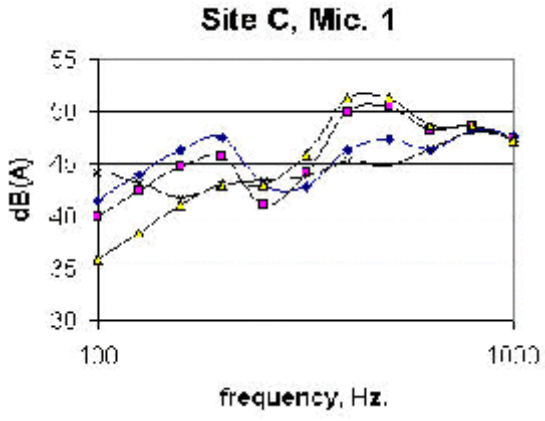

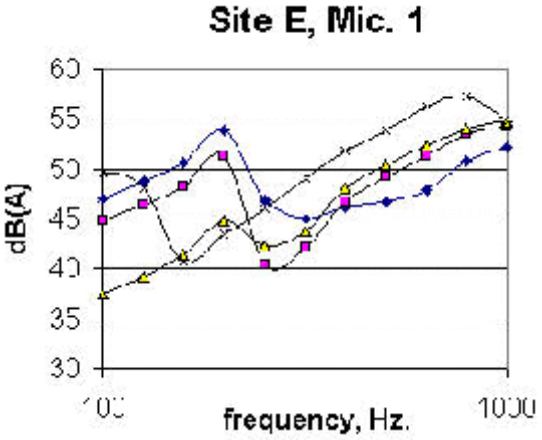

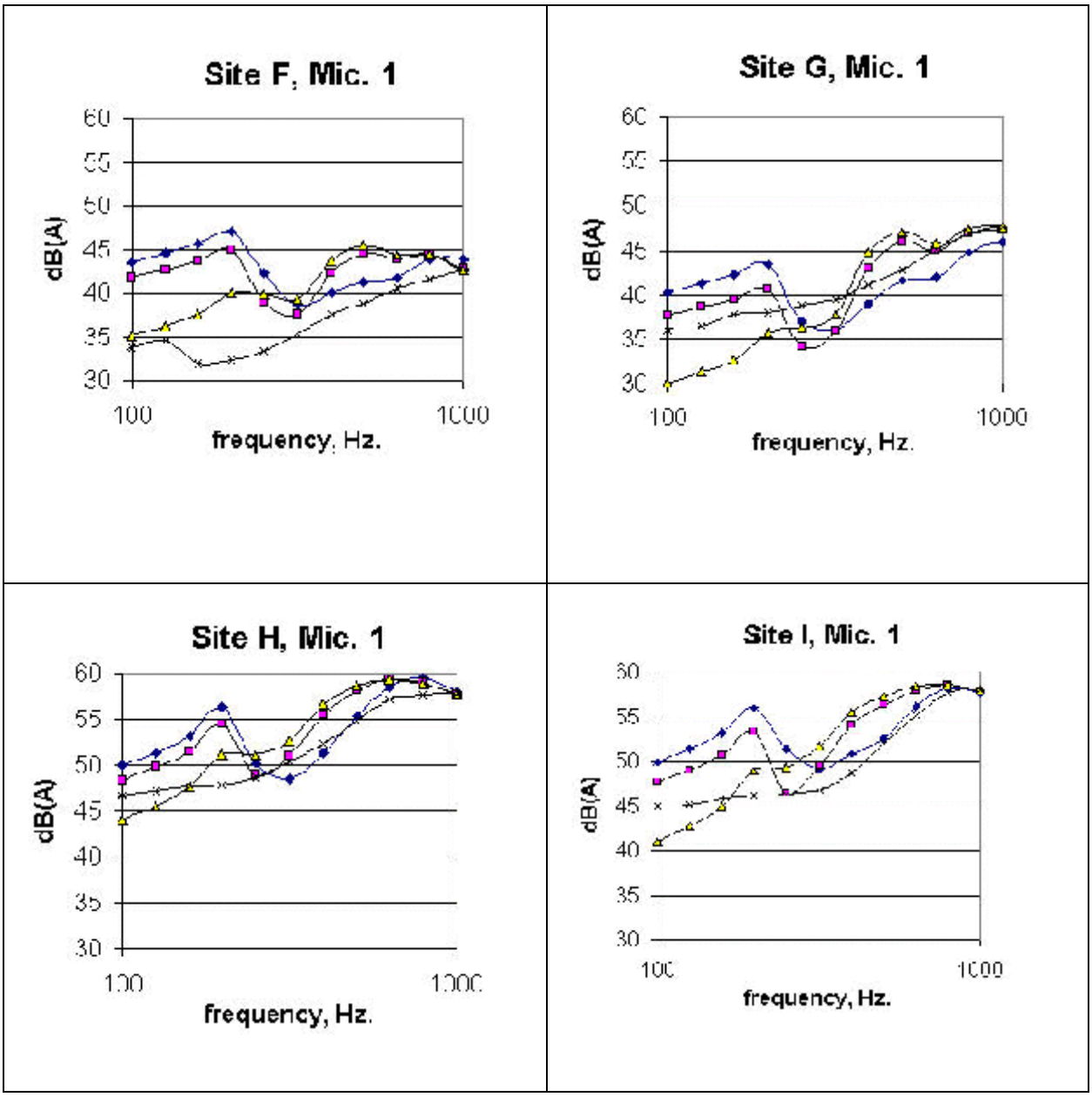
Site F, Mic. 1
dB(A)
60
55
50
45
40
35
30
100
1000
frequency, Hz.
Site G, Mic. 1
dB(A)
60
55
50
45
40
35
30
100
1000
frequency, Hz.
Site H, Mic. 1
dB(A)
60
55
50
45
40
35
30
100
1000
frequency, Hz.
Site I, Mic. 1
dB(A)
60
55
50
45
40
35
30
100
1000
frequency, Hz.

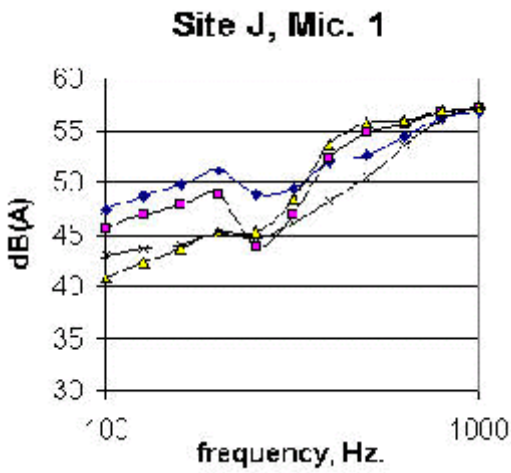
Site J, Mic. 1
dB(A)
60
55
50
45
40
35
30
100
1000
frequency, Hz.

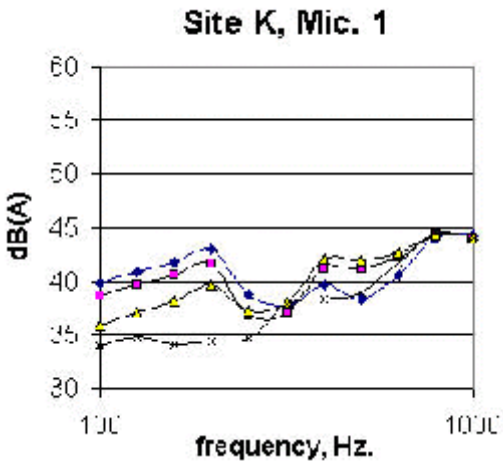
Site K, Mic. 1
dB(A)
60
55
50
45
40
35
30
100
1000
frequency, Hz.

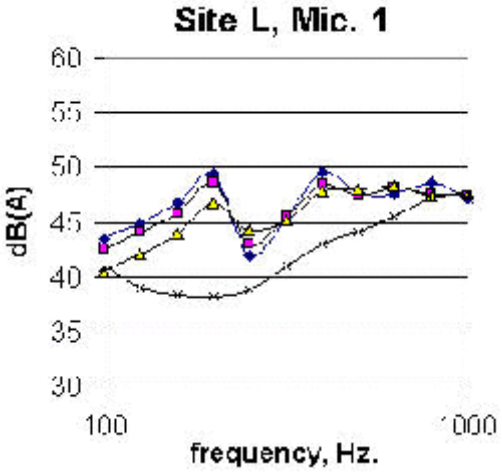
Site L, Mic. 1
dB(A)
60
55
50
45
40
35
30
100
1000
frequency, Hz.

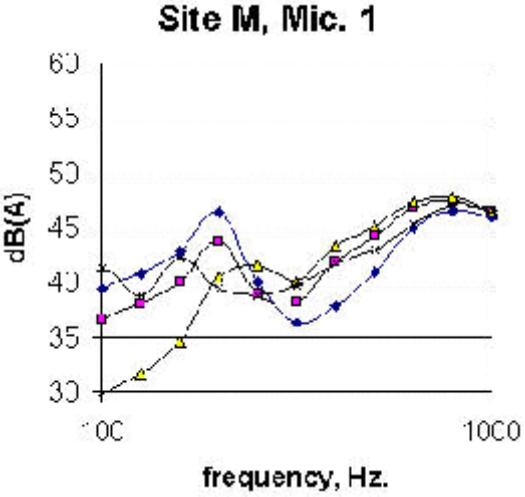
Site M, Mic. 1
dB(A)
60
55
50
45
40
35
30
100
1000
frequency, Hz.

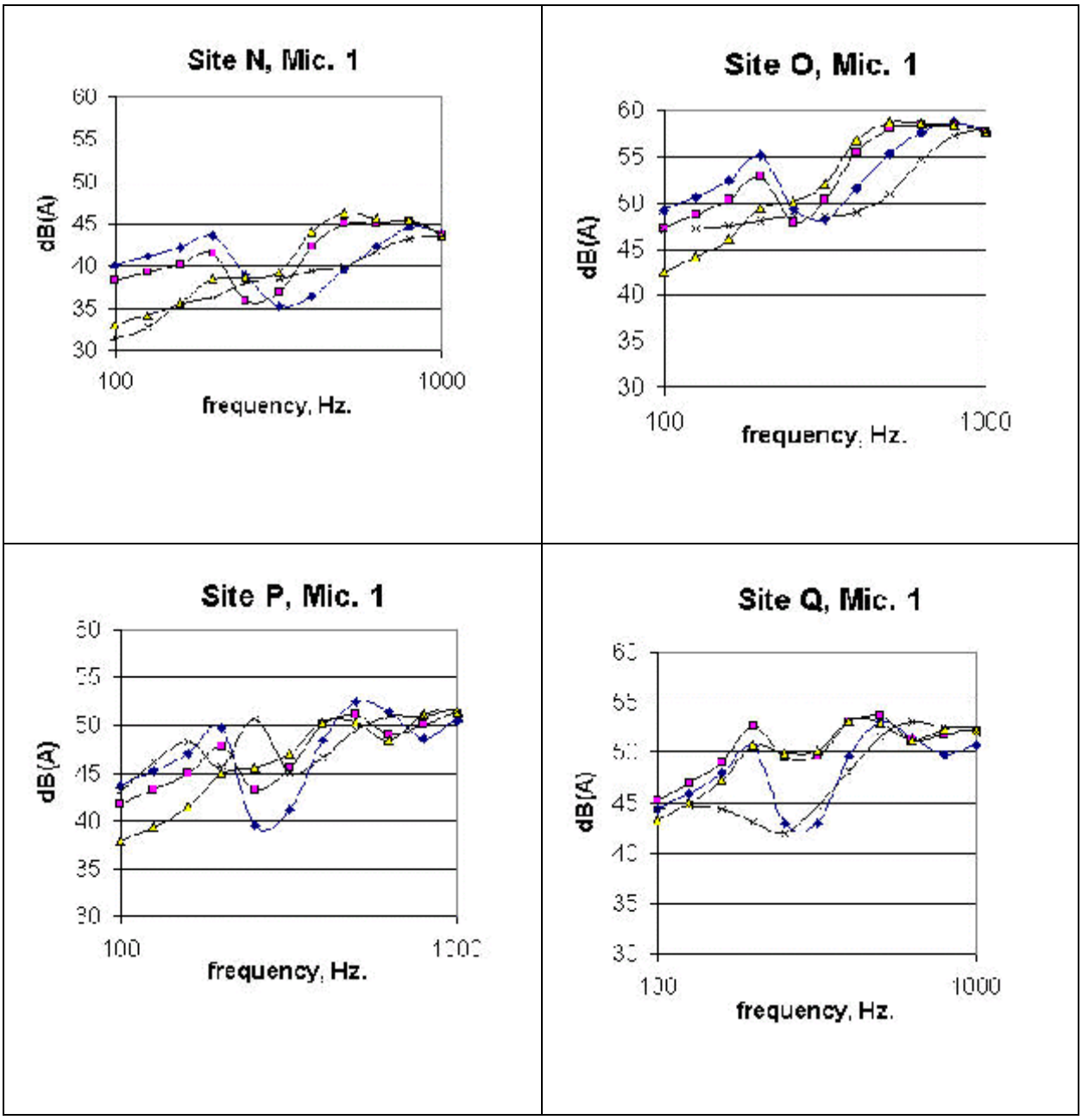
Site N, Mic. 1
dB(A)
60
55
50
45
40
35
30
100
1000
frequency, Hz.
Site O, Mic. 1
dB(A)
60
55
50
45
40
35
30
100
1000
frequency, Hz.
Site P, Mic. 1
dB(A)
50
45
40
35
30
100
frequency, Hz.
Site Q, Mic. 1
dB(A)
45
100
1000
frequency, Hz.

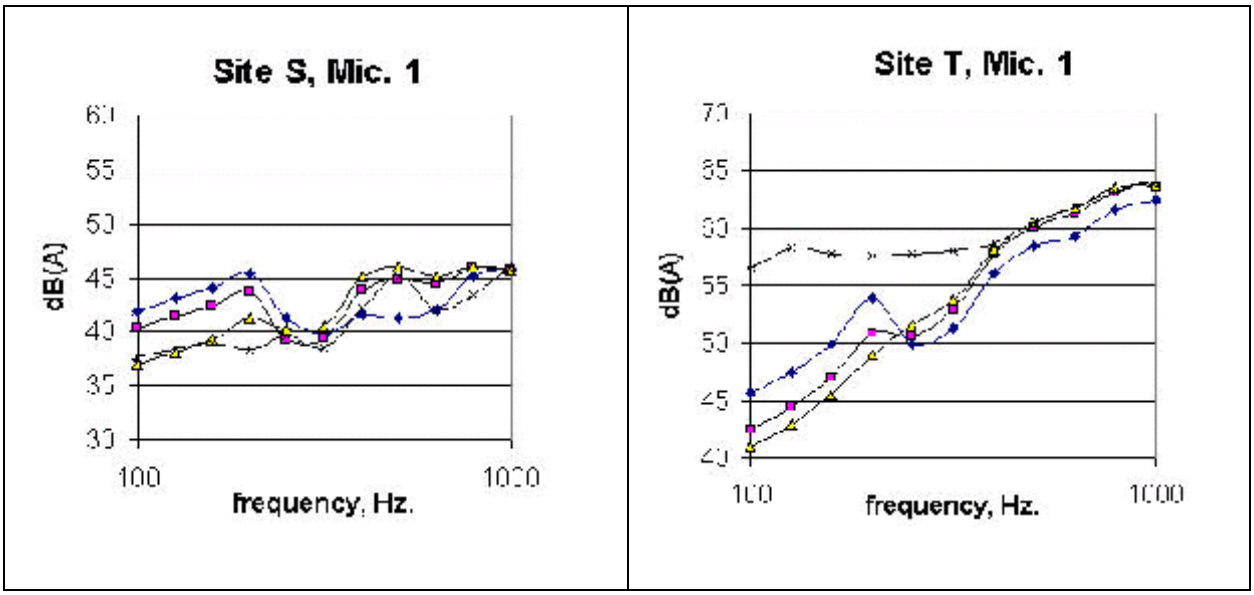

Ground Dip Plots for all Sites: Microphone Position 4

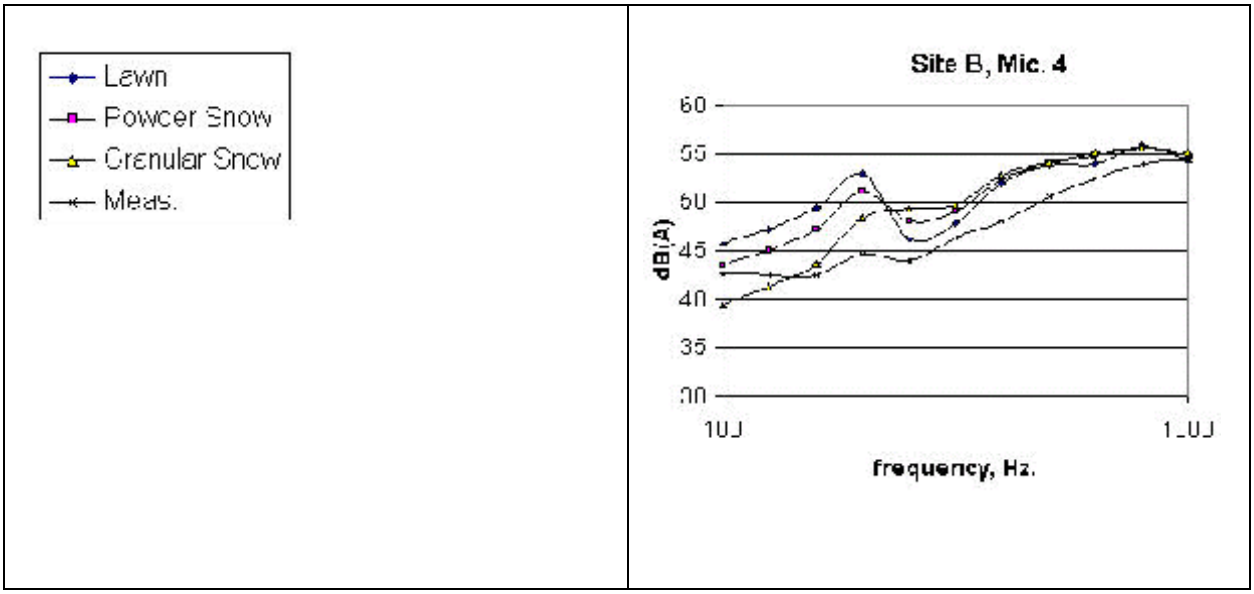

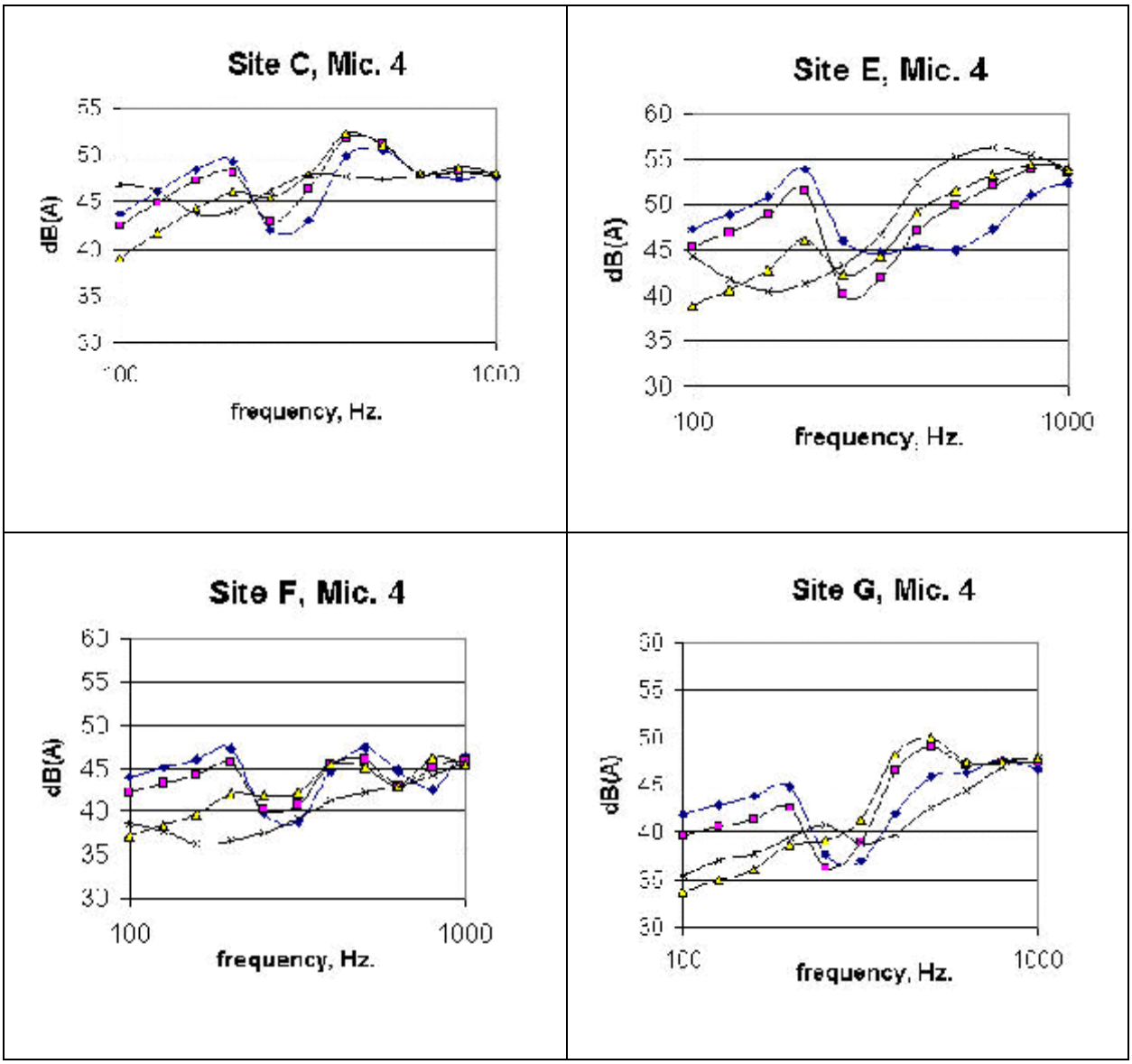
Site C, Mic. 4
dB(A)
55
50
45
40
35
30
100
1000
frequency, Hz.
Site E, Mic. 4
dB(A)
60
55
50
45
40
35
30
100
1000
frequency, Hz.
Site F, Mic. 4
dB(A)
60
55
50
45
40
35
30
100
1000
frequency, Hz.
Site G, Mic. 4
dB(A)
60
55
50
45
40
35
30
100
1000
frequency, Hz.

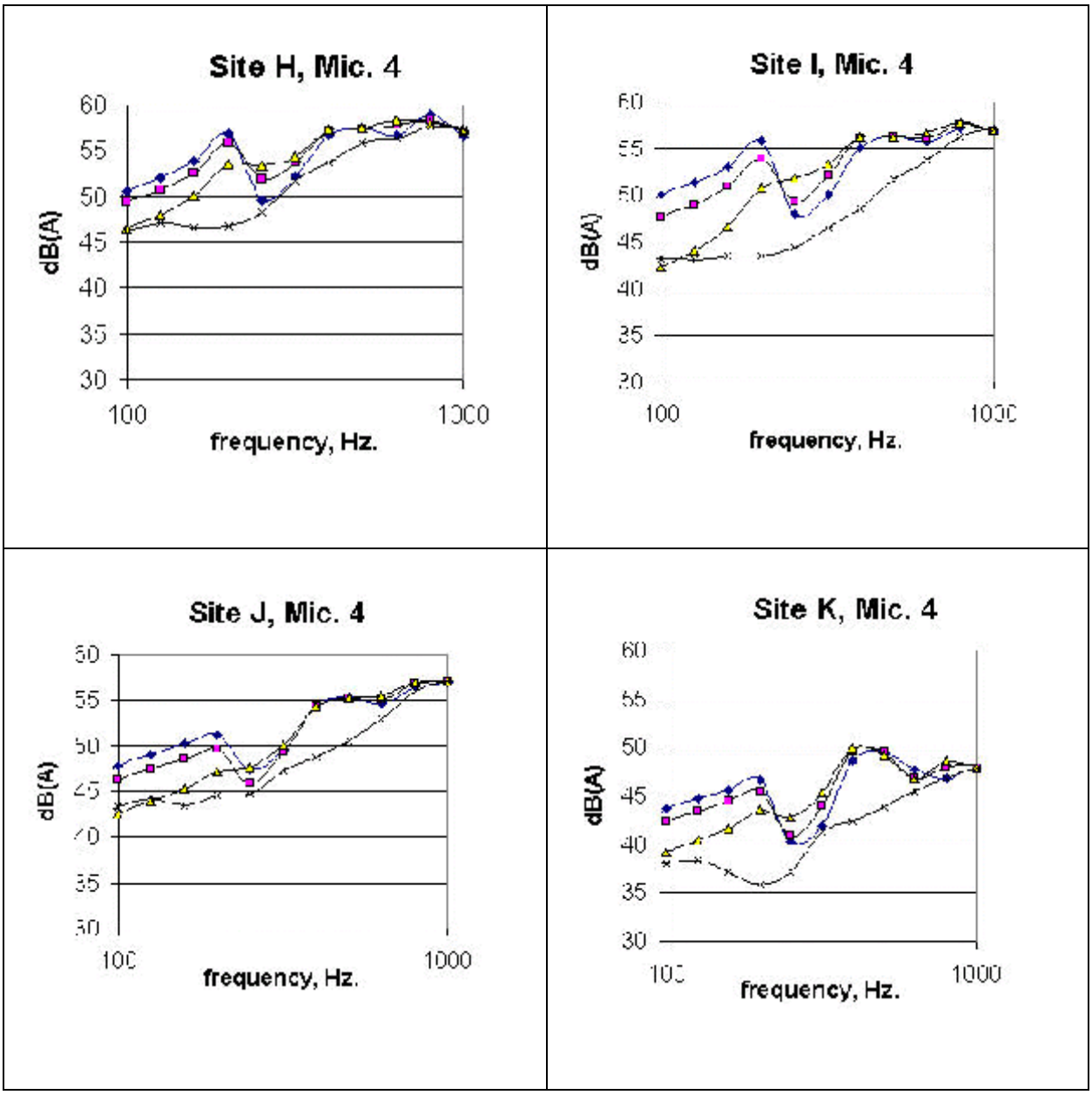
Site H, Mic. 4
dB(A)
60
55
50
45
40
35
30
100
1000
frequency, Hz.
Site I, Mic. 4
dB(A)
60
55
50
45
40
35
30
100
1000
frequency, Hz.
Site J, Mic. 4
dB(A)
60
55
50
45
40
35
30
100
1000
frequency, Hz.
Site K, Mic. 4
dB(A)
60
55
50
45
40
35
30
100
1000
frequency, Hz.

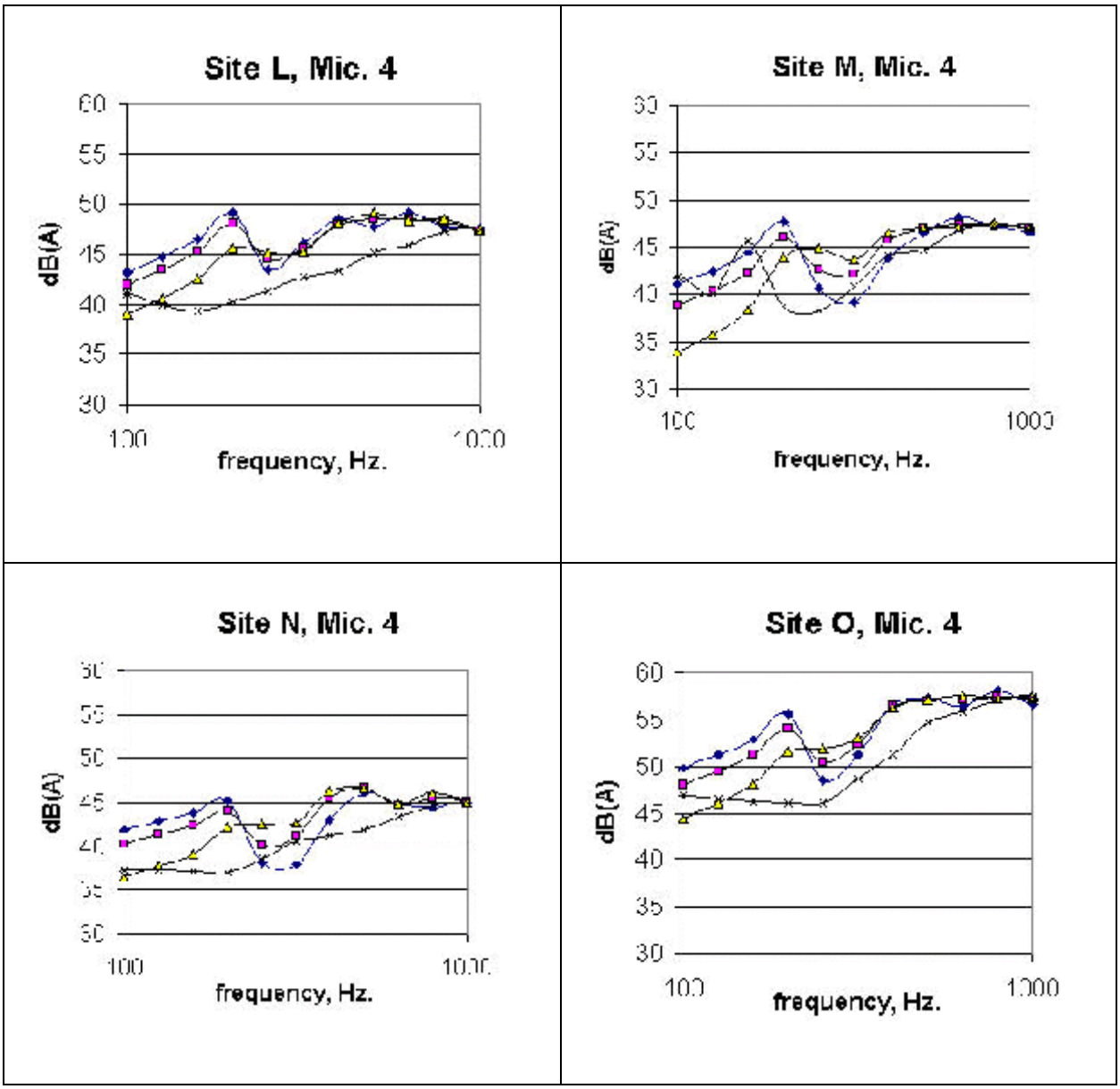
Site L, Mic. 4
dB(A)
60
55
50
45
40
35
30
100
1000
frequency, Hz.
Site M, Mic. 4
dB(A)
60
55
50
45
40
35
30
100
1000
frequency, Hz.
Site N, Mic. 4
dB(A)
100
1000
frequency, Hz.
Site O, Mic. 4
dB(A)
60
55
50
45
40
35
30
100
1000
frequency, Hz.

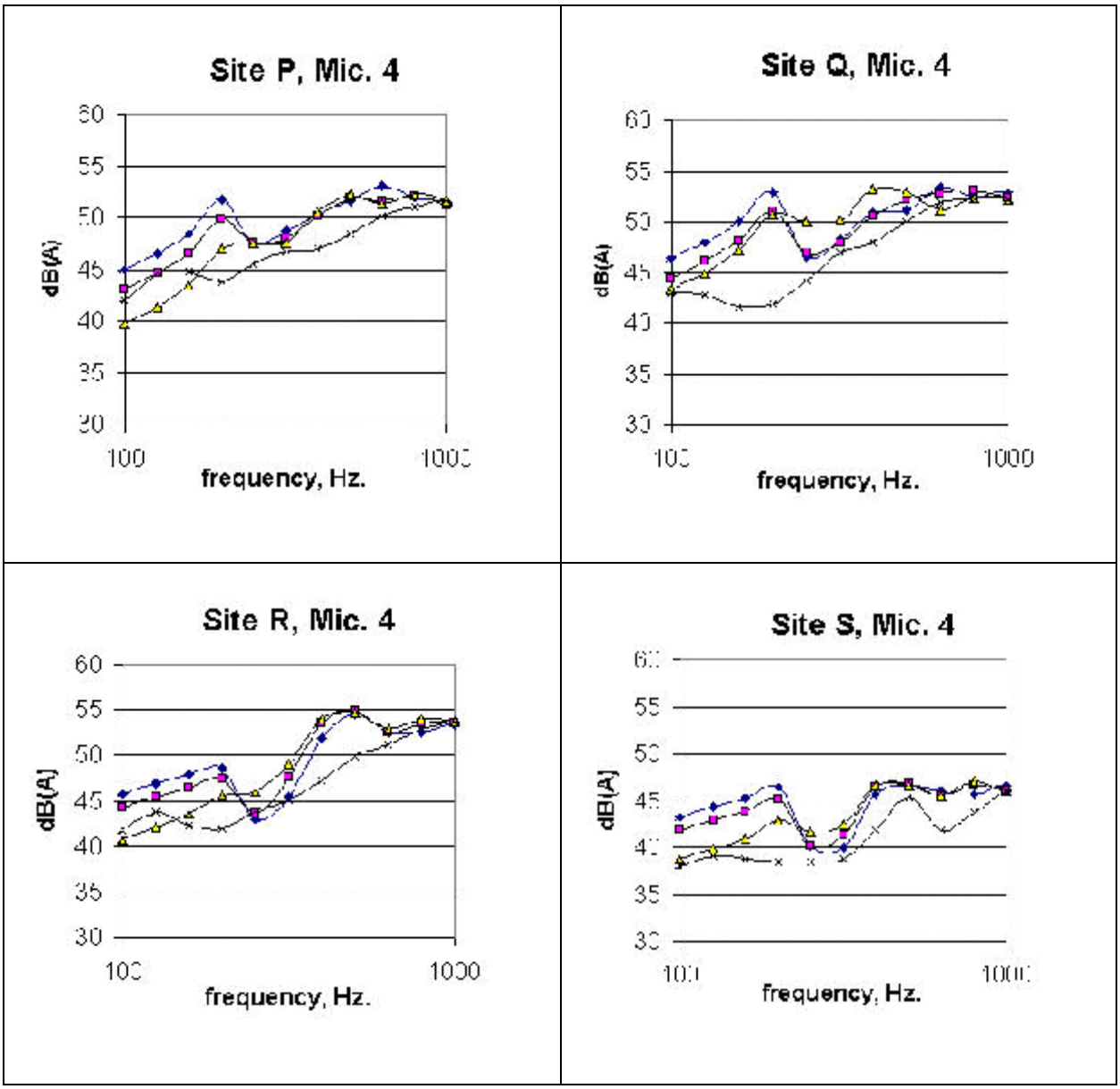
Site P, Mic. 4
dB(A)
60
55
50
45
40
35
30
100
1000
frequency, Hz.
Site Q, Mic. 4
dB(A)
60
55
50
45
40
35
30
100
1000
frequency, Hz.
Site R, Mic. 4
dB(A)
60
55
50
45
40
35
30
100
1000
frequency, Hz.
Site S, Mic. 4
dB(A)
55
50
45
35
100
1000
frequency, Hz.

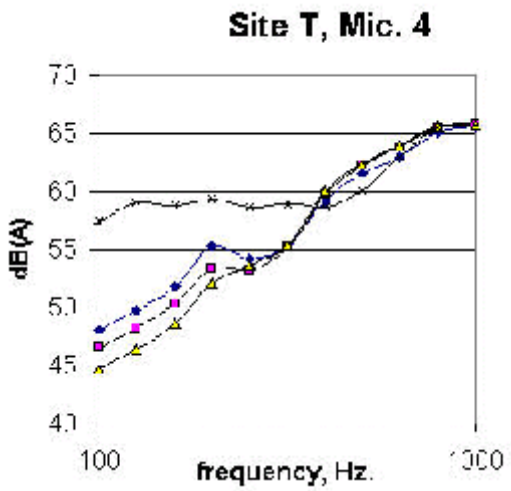
Site T, Mic. 4
70
65
60
55
50
45
40
dB(A)
100
frequency, Hz.
1000

Appendix B

Full Spectra Plots for All Sites (Microphone Positions 1 and 4)

Full Spectra results

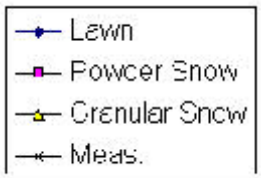

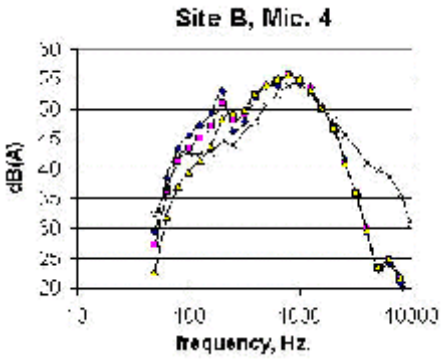

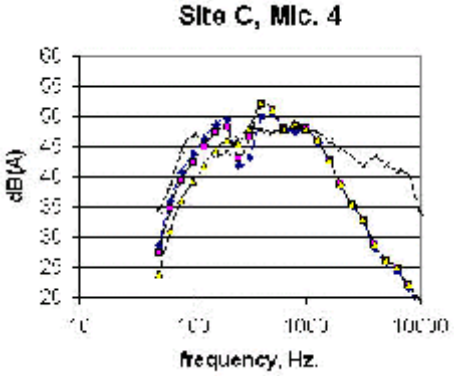

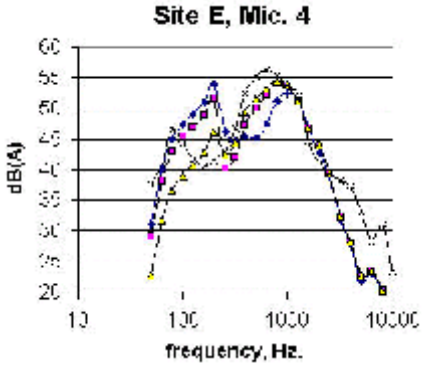

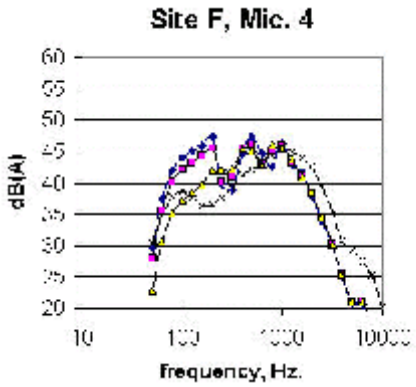

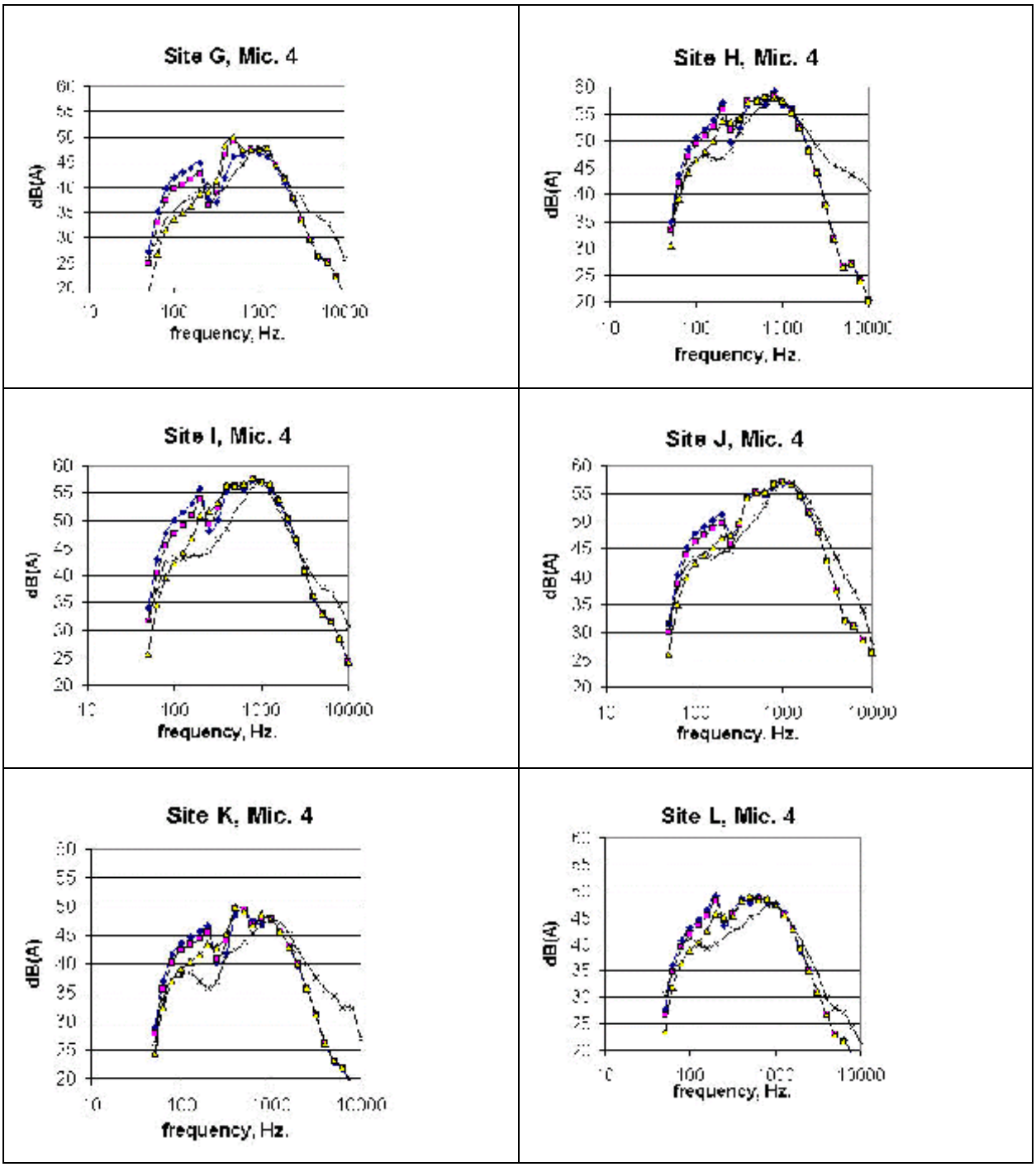
Site G, Mic. 4
dB(A)
frequency, Hz.
Site H, Mic. 4
dB(A)
frequency, Hz.
Site I, Mic. 4
dB(A)
frequency, Hz.
Site J, Mic. 4
dB(A)
frequency, Hz.
Site K, Mic. 4
dB(A)
frequency, Hz.
Site L, Mic. 4
dB(A)
frequency, Hz.

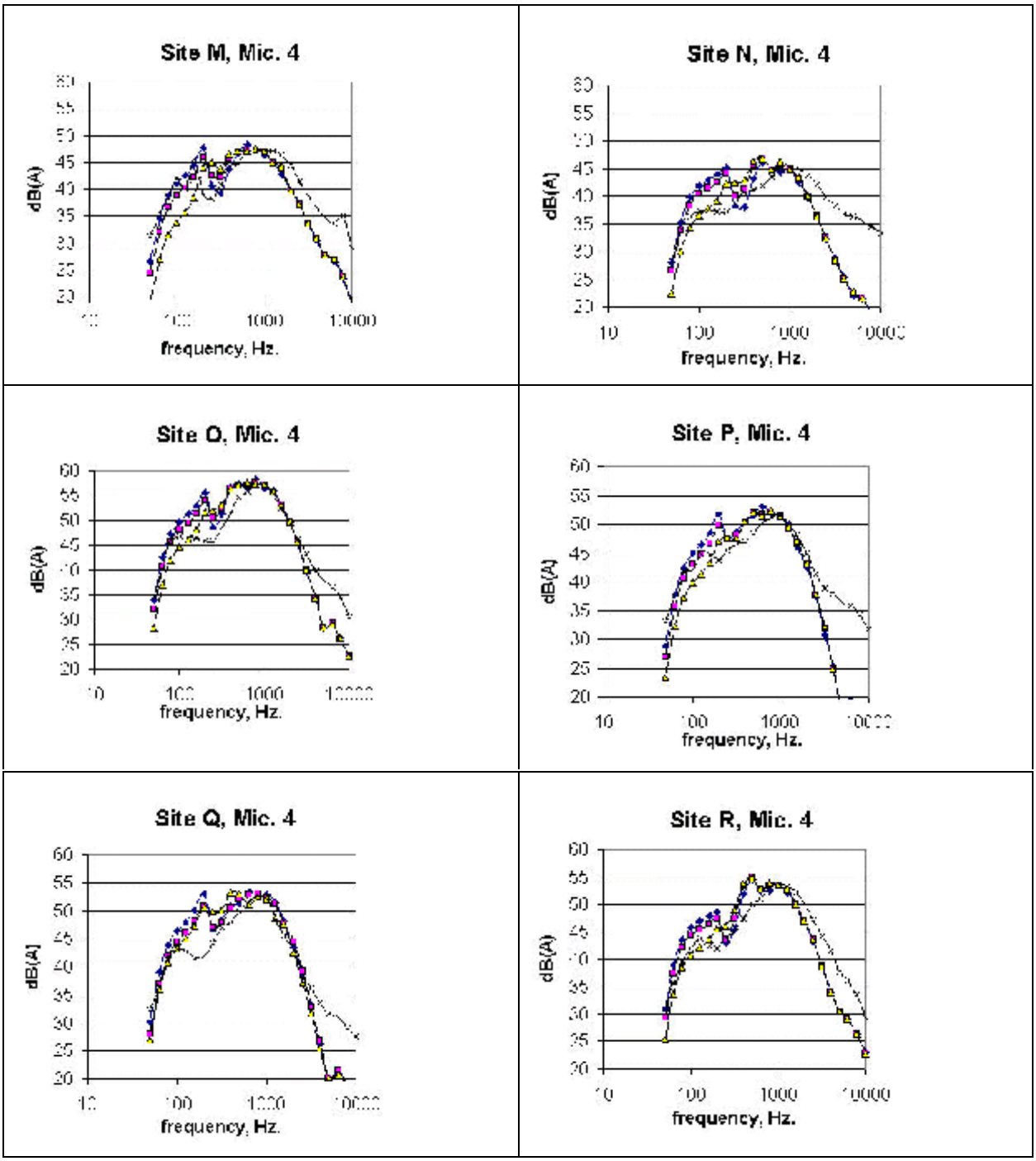
Site M, Mic. 4
dB(A)
frequency, Hz.
Site N, Mic. 4
dB(A)
frequency, Hz.
Site O, Mic. 4
dB(A)
frequency, Hz.
Site P, Mic. 4
dB(A)
frequency, Hz.
Site Q, Mic. 4
dB(A)
frequency, Hz.
Site R, Mic. 4
dB(A)
frequency, Hz.

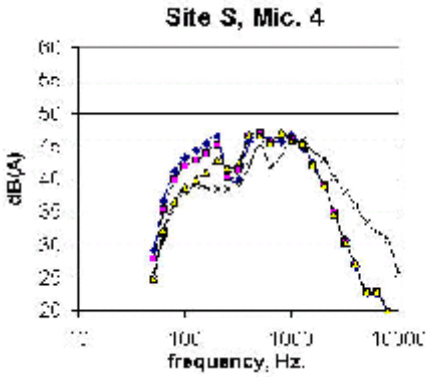
Site S, Mic. 4
dB(A)
frequency, Hz.

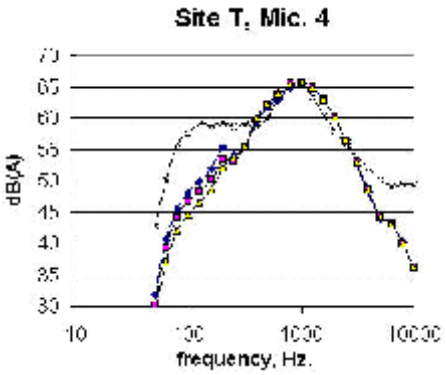
Site T, Mic. 4
dB(A)
frequency, Hz.

Appendix C

Reference Spectra Plots for All Sites (Microphone Positions 7 and 8)

Reference microphone spectra results.

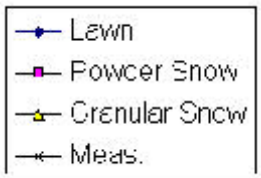

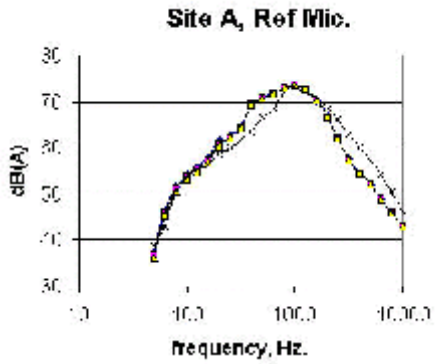

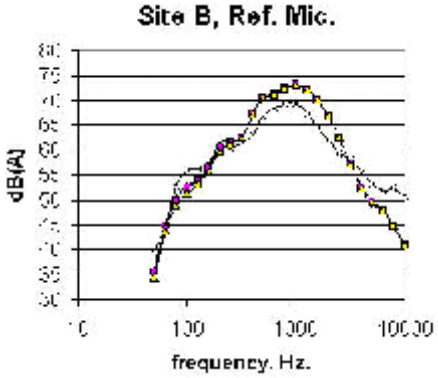

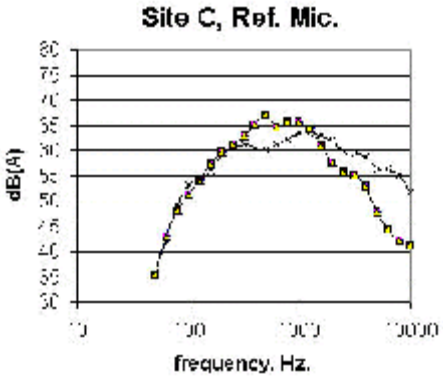

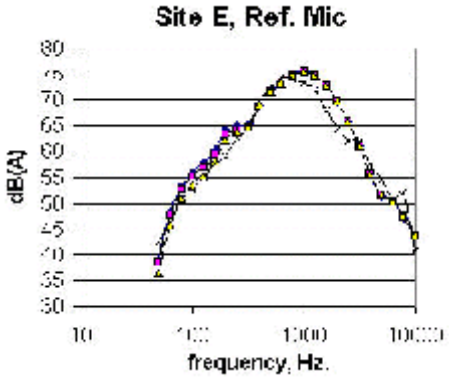

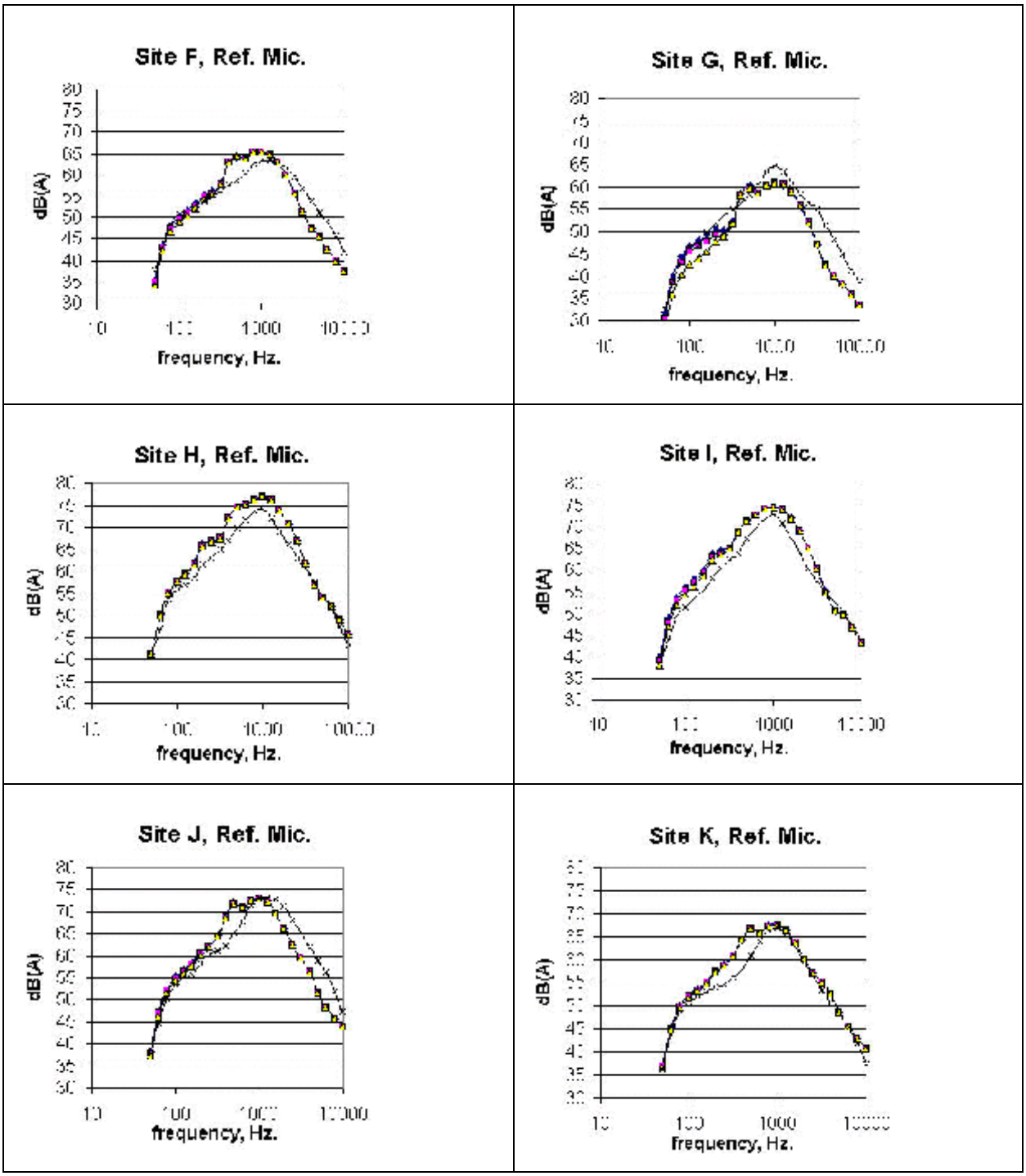
Site F, Ref. Mic.
dB(A)
frequency, Hz.
Site G, Ref. Mic.
dB(A)
frequency, Hz.
Site H, Ref. Mic.
dB(A)
frequency, Hz.
Site I, Ref. Mic.
dB(A)
frequency, Hz.
Site J, Ref. Mic.
dB(A)
frequency, Hz.
Site K, Ref. Mic.
dB(A)
frequency, Hz.

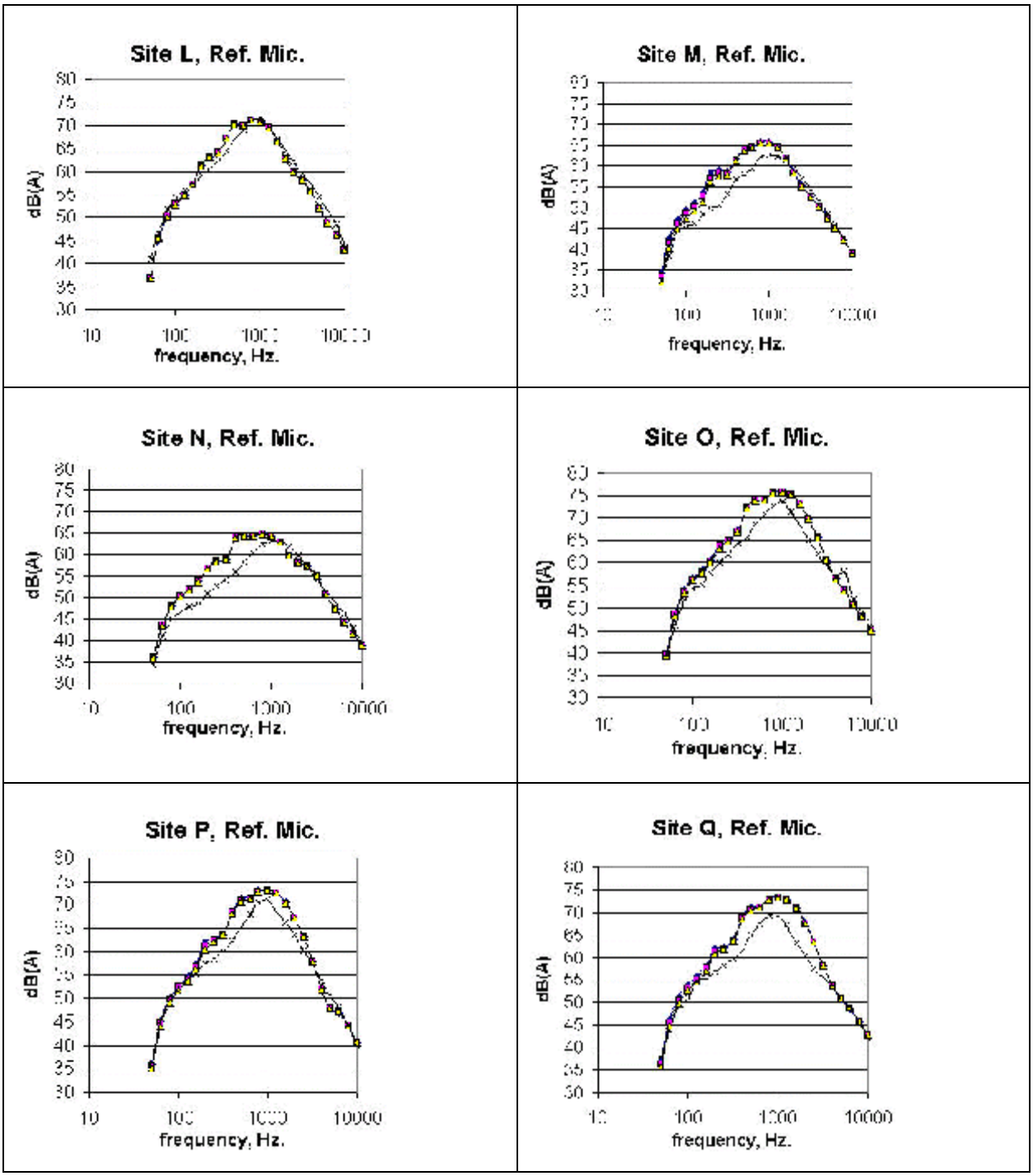
Site L, Ref. Mic.
dB(A)
frequency, Hz.
Site M, Ref. Mic.
dB(A)
frequency, Hz.
Site N, Ref. Mic.
dB(A)
frequency, Hz.
Site O, Ref. Mic.
dB(A)
frequency, Hz.
Site P, Ref. Mic.
dB(A)
frequency, Hz.
Site Q, Ref. Mic.
dB(A)
frequency, Hz.

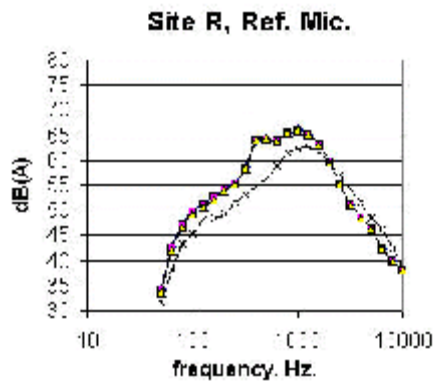
Site R, Ref. Mic.
dB(A)
10
frequency, Hz.

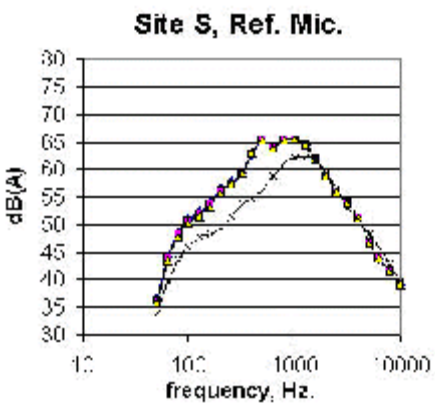
Site S, Ref. Mic.
80
75
70
65
60
55
50
45
40
35
30
dB(A)
10
100
1000
10000
frequency, Hz.

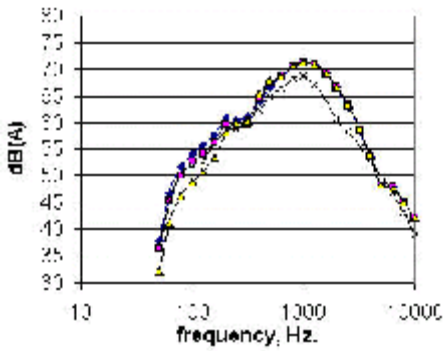
Site T, Ref. Mic.
dB(A)
frequency, Hz.